

See discussions, stats, and author profiles for this publication at: <https://www.researchgate.net/publication/281457039>

# The predator-prey power law: Biomass scaling across terrestrial and aquatic biomes

Article in *Science* · September 2015

DOI: 10.1126/science.aac6284

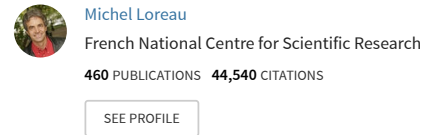
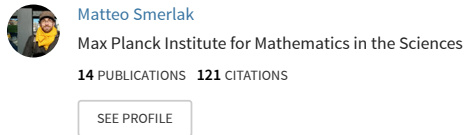
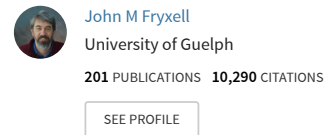
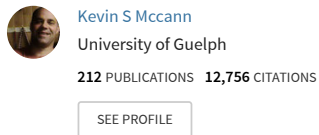
---

CITATIONS  
115

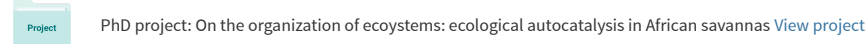
READS  
2,342

---

7 authors, including:



Some of the authors of this publication are also working on these related projects:



## RESEARCH ARTICLE SUMMARY

## MACROECOLOGY

# The predator-prey power law: Biomass scaling across terrestrial and aquatic biomes

Ian A. Hatton,\* Kevin S. McCann, John M. Fryxell, T. Jonathan Davies, Matteo Smerlak, Anthony R. E. Sinclair, Michel Loreau

**INTRODUCTION:** A surprisingly general pattern at very large scales casts light on the link between ecosystem structure and function. We show a robust scaling law that emerges uniquely at the level of whole ecosystems and is conserved across terrestrial and aquatic biomes worldwide. This pattern describes the changing structure and productivity of the predator-prey biomass pyramid, which represents the biomass of communities at different levels of the food chain. Scaling exponents of the relation between predator versus prey biomass and community production versus biomass are often near  $\frac{3}{4}$ , which indicates that very different communities of species exhibit similar high-level structure and function. This recurrent community growth pattern is remark-

ably similar to individual growth patterns and may hint at a basic process that reemerges across levels of organization.

**RATIONALE:** We assembled a global data set for community biomass and production across 2260 large mammal, invertebrate, plant, and plankton communities. These data reveal two ecosystem-level power law scaling relations: (i) predator biomass versus prey biomass, which indicates how the biomass pyramid changes shape, and (ii) community production versus community biomass, which indicates how per capita productivity changes at a given level in the pyramid. Both relations span a wide range of ecosystems along large-scale biomass gradients. These relations can be linked theoret-

ically to show how pyramid shape depends on flux rates into and out of predator-prey communities. In order to link community-level patterns to individual processes, we examined community size structure and, particularly, how the mean body mass of a community relates to its biomass.

**RESULTS:** Across ecosystems globally, pyramid structure becomes consistently more bottom-heavy, and per capita production declines with increasing biomass. These two ecosystem-level patterns both follow power laws with near  $\frac{3}{4}$  exponents and are shown to be robust to different methods and assumptions. These structural and functional relations are linked theoreti-

## ON OUR WEB SITE

Read the full article  
at <http://dx.doi.org/10.1126/science.aac6284>

oretically, suggesting that a common community-growth pattern influences predator-prey interactions and underpins pyramid shape. Several of these patterns are highly regular ( $R^2 > 0.80$ ) and yet are unexpected from classic theories or from empirical relations at the population or individual level. By examining community size structure, we show these patterns emerge distinctly at the ecosystem level and independently from individual near  $\frac{3}{4}$  body-mass allometries.

**CONCLUSION:** Systematic changes in biomass and production across trophic communities link fundamental aspects of ecosystem

structure and function. The striking similarities that are observed across different kinds of systems imply a process that does not depend on system details. The regularity of many of these relations allows large-scale predictions and suggests high-level organization. This community-level growth pattern suggests a systematic form of density-dependent growth and is intriguing given the parallels it exhibits to growth scaling at the individual level, both of which independently follow near  $\frac{3}{4}$  exponents. Although we can make ecosystem-level predictions from individual-level data, we have yet to fully understand this similarity, which may offer insight into growth processes in physiology and ecology across the tree of life. ■

The list of author affiliations is available in the full article online.

\*Corresponding author. E-mail:

i.a.hatton@gmail.com

Cite this paper as I. A. Hatton et al.,

*Science* **349**, aac6284 (2015).

DOI: 10.1126/science.aac6284



**African large-mammal communities are highly structured.** In lush savanna, there are three times more prey per predator than in dry desert, a pattern that is unexpected and systematic. [Photo: Amaury Laporte]

## RESEARCH ARTICLE

## MACROECOLOGY

# The predator-prey power law: Biomass scaling across terrestrial and aquatic biomes

Ian A. Hatton,<sup>1,\*</sup> Kevin S. McCann,<sup>2</sup> John M. Fryxell,<sup>2</sup> T. Jonathan Davies,<sup>1</sup> Matteo Smerlak,<sup>3</sup> Anthony R. E. Sinclair,<sup>4,5</sup> Michel Loreau<sup>6</sup>

Ecosystems exhibit surprising regularities in structure and function across terrestrial and aquatic biomes worldwide. We assembled a global data set for 2260 communities of large mammals, invertebrates, plants, and plankton. We find that predator and prey biomass follow a general scaling law with exponents consistently near  $\frac{3}{4}$ . This pervasive pattern implies that the structure of the biomass pyramid becomes increasingly bottom-heavy at higher biomass. Similar exponents are obtained for community production-biomass relations, suggesting conserved links between ecosystem structure and function. These exponents are similar to many body mass allometries, and yet ecosystem scaling emerges independently from individual-level scaling, which is not fully understood. These patterns suggest a greater degree of ecosystem-level organization than previously recognized and a more predictive approach to ecological theory.

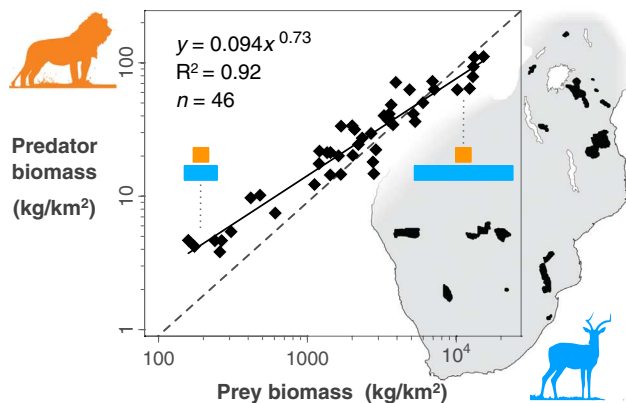
**M**any large-scale patterns in nature follow simple mathematical functions, indicating a basic process with the potential for deeper understanding (1). When the same pattern recurs in different kinds of systems, it urges consideration of their shared properties and provides the opportunity for synthesis across systems (2). Ecology has increasingly observed patterns over very large scales and across levels of organization, from individuals and populations to communities and whole ecosystems (3–8). These patterns depict the boundaries in which life exists and are often highly conserved across taxa and types of communities. This points either to intrinsic characteristics of the individual, such as shared ancestry or energetic constraints (5, 6), or else extrinsic factors, such as the way that many individuals are aggregated, grow, and interact (1, 7). The challenge in ecology, as in many fields, is to link large-scale patterns to finer-grain processes (1, 4).

Here, we present a pattern that follows a simple function and recurs across a variety of ecosystem types in different biomes worldwide. The pattern is only observed over large aggregations of individuals and appears to emerge uniquely at the ecosystem level. We do not know why this

pattern occurs, because it is not predicted by current theoretical models and, as far as we can detect, is unexpected from lower-level structure. What is surprising is that the same pattern recurs systematically in different places, including grasslands, forests, lakes, and oceans. Our analysis has its basis in empirical data drawn from more than 1000 published studies, many of which are cross-system meta-analyses (9–33) (materials and methods, section M1, A to C). In total, we bring together biomass and production measurements for tens of thousands of populations over 2260 ecosystems in 1512 distinct locations globally. Our approach is similar to a number of other large-scale cross-system meta-analyses (10, 19–21, 29–42), allowing comparisons to previous work.

**Fig. 1. African predator-prey communities exhibit systematic changes in ecosystem structure.**

Predators include lion, hyena, and other large carnivores (20 to 140 kg), which compete for large herbivore prey from dik-dik to buffalo (5 to 500 kg). Each point is a protected area, across which the biomass pyramid becomes three times more bottom-heavy at higher biomass. This near  $\frac{3}{4}$  scaling law is found to recur across ecosystems globally.



<sup>1</sup>Department of Biology, McGill University, Montréal, Québec H3A 1B1, Canada. <sup>2</sup>Department of Integrative Biology, University of Guelph, Guelph, Ontario N1G 2W1, Canada.

<sup>3</sup>Perimeter Institute for Theoretical Physics, Waterloo, Ontario N2L 2Y5, Canada. <sup>4</sup>Biodiversity Research Centre, University of British Columbia, Vancouver, British Columbia V6T 1Z4, Canada. <sup>5</sup>Tanzania Wildlife Research Institute, P.O. Box 661, Arusha, United Republic of Tanzania. <sup>6</sup>Centre for Biodiversity Theory and Modeling, Experimental Ecology Station, CNRS, 09200 Moulis, France.

\*Corresponding author. E-mail: i.a.hatton@gmail.com

We began by considering the predator-prey biomass power law in African savanna, shown in Fig. 1, which serves to identify key properties of this more general phenomenon. The pattern describes relative changes in the shape of the “Eltonian” pyramid of biomass, which represents how total biomass is distributed across communities at different trophic levels in the food chain (43–45). In any given environment, the pyramid often exhibits a consistent shape, called the trophic structure, but in different environments, the same communities of species may be in quite different relative proportions (39–42). That is, pyramid shape may change with size, which can be described by the predator-prey power law exponent  $k$ .

Power laws are simple functions of the form  $y = cx^k$ , where  $c$  is the coefficient ( $y$  value at  $x = 1$ ) and  $k$  is the dimensionless scaling exponent (1, 2). On logarithmic axes, power laws follow a straight line with slope  $k$  but on ordinary axes may curve up ( $k > 1$ ) or down ( $k < 1$ ). The slope  $k$  of the relation of the log of predator biomass versus the log of prey biomass identifies the relative change in the shape of the pyramid (Fig. 2). An exponent  $k > 1$  means that the pyramid becomes relatively more top-heavy at higher biomass and is predicted by top-down control of predators on prey (41, 42, 46–48) (appendix S1). An exponent  $k = 1$  indicates that pyramid shape remains constant and is predicted by bottom-up control, whereby a constant fraction of biomass is produced and transferred to each successively higher trophic level (8, 41, 42, 49) (appendix S1). Last,  $k < 1$  indicates that the pyramid becomes relatively more bottom-heavy at higher biomass (Fig. 2).

We show that the shape of the predator-prey biomass pyramid becomes systematically more bottom-heavy as pyramid size increases along a biomass gradient. Similar changes are also observed for per capita productivity with biomass, suggesting a basic link between aspects of ecological structure and function. Our findings thus reveal highly conserved patterns in pyramid size, shape, and growth across different kinds of ecosystems. In particular, community production-biomass scaling is commonly near  $k = \frac{3}{4}$  across

different types of ecosystems and is thus curiously similar to individual production-body mass allometry. This may suggest a similar process recurs across levels of organization.

### Why are there not more lions?

Across African savanna ecosystems (Fig. 1), the total biomass of large carnivores follows a consistent relation to the total biomass of their herbivore prey. The exponent is  $k = 0.73$ , which is sublinear ( $k < 1$ ), and indicates that the trophic pyramid becomes relatively more bottom-heavy at higher biomass. From the dry Kalahari desert to the teeming Ngorongoro Crater, there are threefold fewer predators per pound of prey, which leads to the question: where prey are abundant, why are there not more lions?

### Trophic structure in African savanna

The African predator-prey pattern is remarkably systematic given how it is constituted ( $R^2 =$

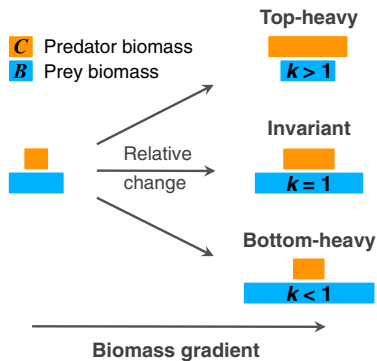


**Fig. 2. The predator-prey power law exponent  $k$  describes relative changes in pyramid shape.**

The slope  $k$  (from  $\log C = k \log B + \log c$ ) identifies how the predator-prey ratio changes along a biomass gradient. Top-heavy and bottom-heavy refer to relative tendencies at higher biomass.

0.92; Fig. 1). Data derive from 190 studies that reported population density in 23 protected areas at different points in time (section M2A). These counts cover the dominant species of large carnivores (wild dog, cheetah, leopard, hyena, and lion) and their characteristic herbivore prey [5 to 500 kg; 27 species (50, 51)]. The population density (numbers of individuals per unit area) of these species vary over 3 to 4 orders of magnitude (Fig. 3A), but, when aggregated into trophic communities within their respective ecosystems, the variability collapses along a highly regular power law (Fig. 1). The observed change in pyramid shape is unexpected given that trophic communities maintain a near constant size structure. The mean body mass, which is the total biomass divided by the total numerical density (52), averages over all individuals and provides an indication of community size structure. Both carnivore and herbivore mean body mass scale with biomass near exponents  $k = 0.03$  (Fig. 3B), indicating that size structure is nearly invariant and that both the pyramids of biomass and the pyramid of numbers (numerical density) change in similar ways (section M2B) (43–45). Both the diversity and the frequency of different size classes are also nearly invariant, so that most species have similar relative frequencies across the biomass gradient (histograms in Fig. 3B). The carnivore-to-herbivore body mass ratio is thus constant even as their biomass ratio declines dramatically (Fig. 3C).

Declines in the predator-prey biomass ratio can be tested by comparing the relation to the null hypothesis of an invariant pyramid shape ( $k = 1$ ). The dashed line in Fig. 1 is the prediction that 1 kg of predator varies with every 111 kg of prey (53). This implies some form of bottom-up control, whereby as prey double, we expect predators to double. In Fig. 3C, the  $y$  axis is trans-

formed to the predator-prey biomass ratio, giving a null exponent  $k = 0$ . In contrast to the null hypothesis, the observed predator-prey biomass ratio exhibits highly significant declines ( $P$  value  $< 10^{-9}$ ), a pattern that has been observed independently in separate studies (9–12) and is robust to a variety of assumptions (section M2B). This pattern, however, cannot be predicted from population or community structure (Fig. 3, A and B), and, as far as we are aware, there is no current theoretical basis for expecting such changes in trophic structure (appendix S1). Large-mammal time series over the past 50 years in several of these systems show that communities are near steady state, even as component populations fluctuate and largely compensate with one another, for a more regular central tendency at the community level (section M2C). The predator-prey pattern thus appears to emerge uniquely at the ecosystem level by aggregating over large numbers of individuals.

### Linking trophic structure and function

If we cannot predict this pattern from lower-level structure, what high-level function might be operating? What flux rates into or out of each trophic community may be shaping trophic structure? For systems near steady state, flux in and out should balance, but flux rates may not be proportional to standing biomass. To investigate the relation between pyramid shape and trophic flux, we consider a simple predator-prey model (Fig. 4). Predator biomass  $C$  and prey biomass  $B$  can be thought to depend on two functions: prey produced  $P(B)$  and prey consumed by predators  $Q(B, C)$ . This model framework includes models going back to Lotka-Volterra, depending on how  $P$  and  $Q$  functions are specified (8, 41, 42, 46–49, 54–57). The model can thus be adapted to different trophic levels in different kinds of systems (appendix S1). Because

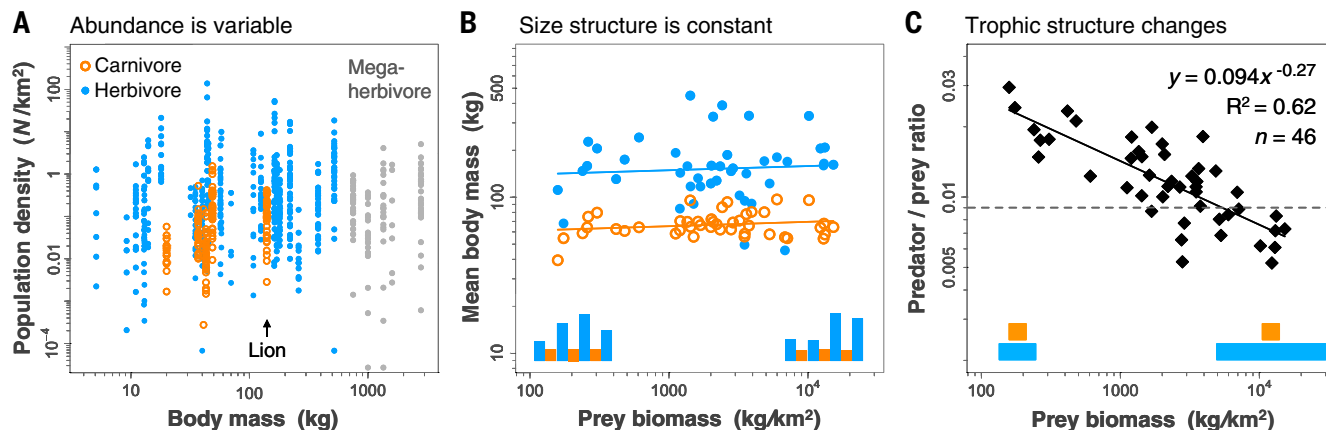


**Fig. 3. Emergent trophic structure in African savanna.** Large mammal abundance is aggregated across systems to show size structure and trophic structure. Trophic structure follows a regular pattern that is not evident from lower-level structure. These data are also shown in Fig. 1 and Fig. 5, A and B. Further details are in section M2. (A) African large mammals vary greatly in density, estimated for 38 species in 23 protected areas at different times. (B) Size structure of predator and prey communities is nearly constant across the biomass gradient. Populations from (A) are aggregated into their

respective predator and prey communities, so that each point is an ecosystem. Mean body mass averages over all individuals in each community (both slopes are  $k = 0.03$  and are not significant). Relative frequencies of different size classes are also near constant, as shown by histograms (bars sum to 1). (C) Carnivore-to-herbivore biomass ratios show significant declines at greater prey biomass ( $P$  value  $< 10^{-9}$ ). Data are as in Fig. 1 but show the predator/prey ratio, which changes threefold across the biomass gradient.

$$\frac{dC}{dt} = gQ - mC$$

$$\frac{dB}{dt} = P - Q$$

**Fig. 4. A predator-prey model (**C**, **B**) with two functions (**P**, **Q**).** Different models are specified based on the functions for prey production  $P(B)$  and prey consumption by predators,  $Q(B,C)$ . Predator production,  $gQ$ , depends on the growth efficiency  $g$  in converting consumption into offspring. Predator loss is  $mC$ , where  $m$  is mortality rate.

we believe African large mammal communities to be near steady state ( $C^*$ ,  $B^*$ ), the predator-prey power law can be expressed as

$$C^* = cB^{*k}$$

where  $c$  is the predator-prey coefficient (in Fig. 1,  $c = 0.094 \text{ kg}^{1-k}$  and  $k = 0.73$ ). We thus seek  $P$  and  $Q$  functions that give rise to this structural pattern. At equilibrium, both equations in Fig. 4 can be set to zero, and we can substitute the prey equation ( $Q^* = P^*$ ) into the predator equation ( $C^* = gQ^*/m$ ) (where  $g$  is the predator growth efficiency and  $m$  is the predator mortality rate), giving  $C^* = gP^*/m$ . To obtain  $C^* = cB^{*k}$  above, prey production may scale in the same way with prey biomass, which can be expressed as

$$P = rB^k$$

Here  $r$  is the prey production coefficient (units  $\text{kg}^{1-k}/\text{time}$ ), and  $k$  is assumed to be 0.73. The predator-prey coefficient is thus

$$c = rg/m$$

Regardless of how consumption  $Q$  is specified, trophic structure should depend on lower trophic productivity,  $P$ , according to a simple relation of flux rates. On the left of the equality is the predator-prey coefficient  $c$ , which influences pyramid shape, whereas on the right are parameters for flux rates into and out of each trophic community. Clearly, the dynamic interactions of five carnivore species and many more species of prey across vast areas of the continent cannot be captured by two differential equations. This coarse-grained description, however, focuses on a few key flux rates and brings dynamical perspective to the question of what is shaping trophic structure. We have tested this theoretical prediction ( $c = rg/m$ ) for African large mammals, estimating their community rate parameters ( $r$ ,  $g$ , and  $m$ ) independently from the fitted coefficient in Fig. 1, and find close correspondence (appendix S2). This suggests a link between trophic structure and the production function. Specifically, where prey are abundant, they appear to reproduce at consistently lower rates, which in turn influences the biomass of predators. Lion abundance, for example, appears

to depend on the productivity of the prey community, which exhibits a systematic form of density dependence, but also on the densities of other predators, with which lions are compensatory. The regularity of this pattern suggests high-level organization and possibly complex regulatory pathways, which only more detailed study can elaborate. But how general are these structural and functional patterns across other kinds of ecosystems?

### Biomass scaling globally

Predator-prey biomass scaling is not unique to the African savanna and is found to recur across a variety of other kinds of ecosystems. Our model suggests this pattern is underpinned by similar production-biomass scaling (Fig. 4). Although data are not available for the same ecosystems to test this connection directly, these two scaling relations exhibit similar exponents near  $k = 3/4$  across terrestrial and aquatic ecosystems. This suggests that a common community growth pattern may be shaping biomass pyramids across distinct ecosystem types.

### Empirical findings

Predator and prey biomass follow a power law with a sublinear exponent ( $k < 1$ ) across several terrestrial and aquatic biomass gradients. Tiger and wolf biomass over their respective continents both scale to prey biomass with exponents near  $k = 3/4$  (Fig. 5, C and D) (13–17). These carnivores represent a dominant part of the large predator community, comparable to lion and hyena populations (Fig. 5, A and B). Similarly, zooplankton and phytoplankton biomass follow near  $3/4$  scaling patterns across lakes and oceans and through time (Fig. 5, E to H) (18–22). A number of studies have reported the same qualitative declines in predator-prey ratios across diverse environments (14, 17, 19–22, 38, 40–42, 58–64) (section M3), suggesting a widespread phenomenon.

Similar scaling is also observed for community production-biomass relations in grasslands (23–25), broadleaf and coniferous forests (26–28), seagrass beds (29), and algal (18) and invertebrate communities (30) (Fig. 5, I to O; section M3, I to O; and table S1). Exceptions to this pattern exist where multiple trophic groups are combined. Fish (Fig. 5P), for example, combine benthivores and planktivores, as well as piscivores, at a higher trophic level (31, 32). Although data are few, when these trophic groups are considered separately, lower-trophic groups scale sublinearly [ $k$  ranges from 0.74 to 0.81 (33)], whereas piscivores exhibit near-linear scaling ( $k = 1.1$ ; section M3P). It is possible that piscivores are dominating the pattern in Fig. 5P, although data among higher trophic levels are generally limited.

This pattern is largely robust to regression methods and is validated by independent data sources. Previous cross-system studies have reported exponents fit by ordinary least squares (10, 19–21, 29–42). As far as we can determine, this is the least biased regression method for the data that we report (section M1D). Although least squares exponents are increasingly under-

estimated with increasing error, alternative methods (e.g., type II) tend to overestimate the exponent (section M1D) and yet are also sublinear ( $k < 1$ ) for all plots, except where data are highly dispersed [Fig. 5, F, G, and L;  $R^2 < 0.5$ ;  $k$  near 1; section M3; (65)]. Nonetheless, we cannot be certain of the exponent value, and even the best-studied ecosystem types do not extend much beyond a two order of magnitude biomass gradient, which may be insufficient to establish power law behavior. Currently available data also do not permit highly standardized community level measurements, so that different biomes may represent different levels of sampling and taxonomic resolution. Despite these limitations, however, declines in  $y/x$  versus  $x$  are highly significant for all variables in Fig. 5, A to O (all  $P$  values  $< 0.01$ ). Similar scaling is also obtained for each of 25 published cross-system data sets (9–30, 66, 67);  $k_{\text{avg}} = 0.72$ ;  $n_{\text{tot}} = 2950$  ecosystems; section M3; table S2), providing independent validation of the pattern. Across terrestrial and aquatic ecosystems, therefore, the predator-prey ratio and per capita production decline significantly at higher biomass, both following similar scaling.

### Theoretical implications

Several cross-system meta-analyses, using similar methods to our own, have shown that herbivore consumption scales near linear ( $k = 1$ ) to primary production (34–37) (section M3Q and table S5). This implies that flux rates into and out of basal communities are roughly proportional across productivity gradients, which may be expected for systems near steady state. Together with these earlier studies (34–37), our empirical findings have implications for ecological theory.

1) Predator-prey scaling is sublinear (Fig. 5, A to H), which indicates that trophic structure is more bottom-heavy at higher biomass. At steady state, this can be expressed as  $C^* = cB^{*k}$ , where  $c$  is the predator-prey coefficient and  $k < 1$ . This equilibrium solution is at odds with common models that assume that prey production  $P$  follows logistic density dependence. These models are often classed as top-down or bottom-up control according to how  $Q$  is specified and predict more top-heavy ( $k > 1$ ) or invariant ( $k = 1$ ) pyramid structures with increasing biomass (8, 41, 42, 46–49) (appendix S1). Classic models can be reconciled with data by introducing the production function described below (2).

2) Production-biomass scaling is sublinear (Fig. 5, I to O) and indicates that per capita growth declines at higher biomass. For prey, this can be expressed as  $P = rB^k$ , where  $r$  is the production coefficient and  $k < 1$ . This production function theoretically yields observed predator-prey scaling (Fig. 4) and implies that, in the absence of predators, prey increase if food is available, but with an ever-diminishing tendency. This is a weaker form of density dependence than logistic, but systematic and possibly scale-free. Model stability is thus found to be extensive in parameter space for different  $Q$  functions

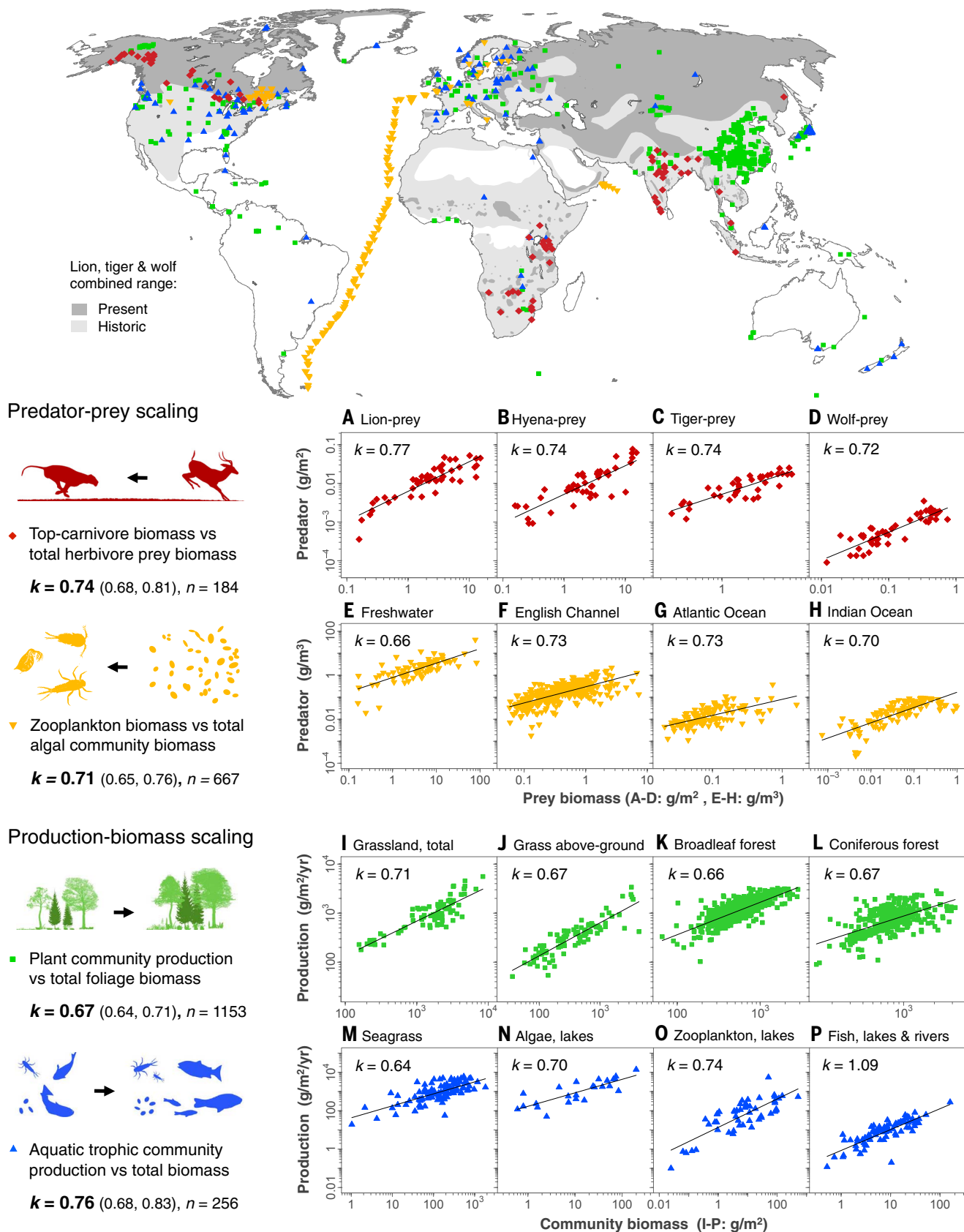


**Fig. 5. Similar scaling links trophic structure and production.** Each point is an ecosystem at a period in time ( $n = 2260$  total from 1512 locations) along a biomass gradient. (A to P) An exponent  $k$  in bold (with 95% CI) is the least squares slope fit to all points  $n$  in each row of plots. Further details are in section M3 and table S1.

(see supplementary text), suggesting that this growth pattern may help to balance trophic interactions across large-scale gradients.

3) The similarity of predator-prey (item 1) and production-biomass (item 2) scaling implies a broadly conserved link between these structural and functional variables. Although our model (Fig. 4) is only a phenomenological description of trophic dynamics, it may provide a first approximation for the link between these two power law coefficients ( $c = rg/m$ ), allowing variables in Fig. 5 to be reformulated in terms of one another for more extensive predictions (e.g., appendix S2). Theory and data thus point to a general community growth pattern that shapes trophic structure in terrestrial and aquatic systems.

But where does this growth pattern originate? Although we cannot be certain of the exponent value, ecosystem-level scaling is often near  $k = \frac{3}{4}$  and evokes a link to individual-level body mass allometry. Many vital characteristics of an individual scale with body mass near  $k = \frac{3}{4}$  (68), including metabolism (5, 6), production (69–72), and consumption (9, 52, 57). This means that, as a body enlarges within a species or across taxa, these rates decline on a per mass basis. Near  $\frac{3}{4}$  body mass exponents appear to be physiologically linked and are widely thought to be energetically constrained (5–7, 71–76). Here, however, we are considering aggregations of many individuals across separate ecosystems, and so it is not clear how the same energetic constraints would apply. Unlike the similarity between predator-prey and production-biomass scaling, which has some theoretical basis (implication 3, above), the similarity between ecosystem and individual scaling does not.

### Links to lower levels

Community production and biomass represents the total individual production and total body mass summed over all individuals within the community, and so we consider the individual production allometry. From microscopic algae up to elephant, maximum individual production exhibits highly robust near  $\frac{3}{4}$  scaling with body mass (Fig. 6 and section M4) (5, 6, 68–76). Individual and community production scaling are thus notably similar, and although there are important exceptions, such as for individual protists (77), this parallel tends to hold across major taxa (Fig. 7) (tables S1 to S3). But maximum individual growth is not the actual individual growth within a community, and so this apparent similarity may be misleading.

### Deductions from size structure

To connect ecosystem- to individual-level processes, we examine community size structure (Fig. 8) and specifically mean body mass versus total biomass (52) (section M5). As in African ecosystems (Fig. 3B), we find that size structure shows few systematic changes across large mammal and forest biomass gradients (Fig. 8, A to C) (13–16, 26, 27). In contrast, at higher aquatic biomass, mean size increases in plankton com-

munities, especially among algae (Fig. 8, D to F) (22, 31, 32, 52). For biomass scaling to be the direct result of body mass allometry, we expect mean body mass to scale with biomass near  $k = 1$ . Changes in plankton size structure, therefore, are not sufficient to account for changes in trophic structure or per capita productivity. We can thus deduce the following (which only partly holds for plankton communities).

1) Ecosystem and individual near  $\frac{3}{4}$  exponents appear to arise independent of changes in size structure. Mean body mass is poorly correlated to community biomass, indicating that their mass exponents are not directly related.

2) Increases in community biomass along a

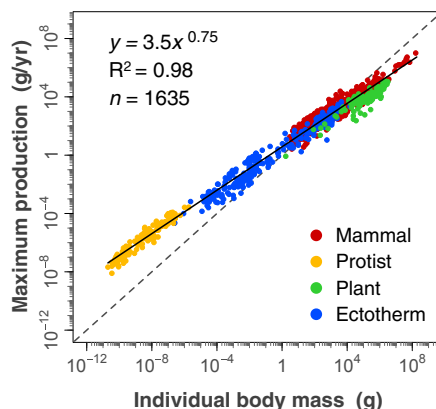


**Fig. 6. Individual production to body mass exhibits near  $\frac{3}{4}$  scaling across taxa.** Maximum individual production includes somatic growth and offspring production. Each point is an individual, representing 1098 species over 127 taxonomic orders. Further details are in section M4 and table S3.

biomass gradient are largely due to increases in population density. Increases in biomass may also be due to increases in diversity but are never solely due to changes in body size.

3) Per capita declines in community production are largely due to density-dependent declines in individual productivity from their maximum potential, shown in Fig. 6.

Size structure thus suggests that the scaling of individual maximum production is independent from that of community production. Instead, individual production appears to systematically decline from its maximum (Fig. 6), with increases in the density of the community in which it resides. We therefore expect to observe maximum individual production only at very low densities, where we can make predictions for community production from individual data. At higher densities, however, community production will likely be overestimated unless density dependent declines in individual production are accounted for. Assuming a biomass exponent

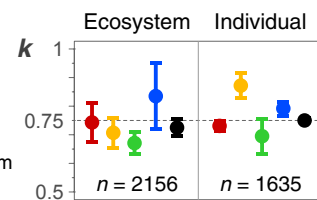


**Fig. 7. Ecosystem and individual growth patterns are similar.** Least squares exponents  $k$  (and 95% CI) for production-mass across ecosystems (from Fig. 5) and individuals (from Fig. 6) are often near  $k = \frac{3}{4}$ . Each exponent estimate is for  $n > 100$  data points. Seagrass data ( $n = 104$ ; Fig. 5M) were excluded. Further details are in section M4.

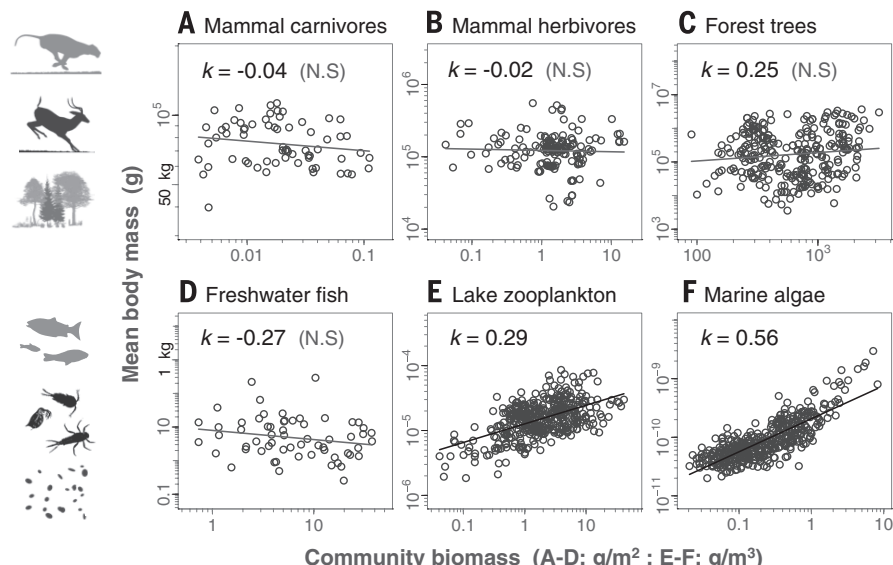


**Fig. 8. Mean body mass is poorly correlated to community biomass except in plankton.** Points are mostly the same as those in Fig. 5. Mean body mass averages over all individuals in a community. The slopes  $k$  in (A) to (D) are not significant (N.S.; all  $R^2 < 0.05$ ), but plankton size structure varies positively with biomass (E and F). Mammal systems (A and B) include data from Fig. 3B. Further details are in section M5 and table S4.

near  $k = \frac{1}{4}$  allows community-level predictions from individual-level data across a biomass gradient (appendix S2).

## Outlook

Size-structure suggests unique emergence of growth scaling at the community and individual levels, and, although we can make high-level predictions from lower-level function, we do not know why growth patterns at different levels are so markedly similar. Models for individual growth scaling going back to the well-known Bertalanffy model assume a dependence on metabolic scaling (73–76). Although our model for prey community growth (Fig. 4) resembles these ontogenetic growth models, we cannot assume the same metabolic rationale. Community growth scaling arises over large aggregations of individuals that often change little in their size structure, which leads us to wonder not only what underpins this pattern in different ecosystems, but how might it recur across levels of organization.

Density-dependent growth has been observed over thousands of populations in diverse taxa (78, 79) and is qualitatively consistent with this growth pattern. Population density is known to influence physiology, community composition, and competition for space. Density-dependent factors can alter reproductive behavior, life history, and metabolism (80, 81); promote self-shading and self-thinning (82, 83); cause changes in size structure and nutritional quality (36–41, 84–86); and trigger interference and territorial aggression (87, 88). What is not known is whether these factors can account for observed scaling exponents, and whether these different factors may have similar effects when aggregated across whole communities. The generality of community-level scaling suggests a process that operates in regular ways and independently of system details. A theory for growth-mass scaling encompassing both individual and ecosystem levels would efficiently unite basic aspects of physiology and ecology.

## Conclusion

Ecosystems exhibit emergent regularities in trophic structure and production dynamics across terrestrial and aquatic biomes of the world (Fig. 5). The predator-prey ratio and per capita community production both significantly decline at higher biomass. Both of these relations follow similar power law scaling, which suggests a conserved link between ecosystem structure and function across diverse systems. Often these patterns are highly regular (e.g., Fig. 1), implying a greater degree of ecosystem-level organization than previously recognized and raising questions about the processes that regulate abundance in ecological communities. We show how sub-linear growth scaling tends to stabilize predator-prey interactions (supplementary text), but further work is needed to understand how specific factors operate in different systems.

Perhaps the most intriguing aspect of these findings is that community and individual growth patterns both follow near  $\frac{1}{4}$  scaling laws (Fig. 7).

Community growth scaling emerges over large numbers of individuals and size structure is often near constant, indicating that similar growth dynamics at the community and individual levels arise independently (Fig. 8). This may point to basic processes that reemerge across systems and levels of organization.

## Materials and methods

A description of our empirical approach and data (Figs. 1 to 5) is outlined below (sections M1 to M5). Materials and methods are supplemented with regression tables S1 to S5 and appendices S1 and S2 (supplementary materials file), as well as raw data and original sources in the data file (database S1), and are available at *Science* Online.

### M1. Empirical approach

#### A. Criteria for inclusion in the database

This study focuses on how ecological structure and dynamics change across ecosystems made of similar species assemblages. This requires data gathered consistently by different studies across large-scale biomass gradients. We focused on relatively distinct trophic communities, rather than ecosystems with more complex feeding relationships. This restricted the kinds of ecosystems that could be considered to currently available data on large mammals, plants, and basal aquatic communities.

All data were sourced from peer-reviewed publications and met the following criteria: (i) Ecosystems were relatively free of human influence or disturbance and were thus representative of natural conditions. (ii) Ecosystems were surveyed over a much larger area than the largest animal home range, so that density estimates were not biased because of local aggregation. (iii) Communities comprised the majority of dominant species and were thus representative of whole trophic communities. Noted exceptions include predator communities in Southeast Asia and North America, represented by a single top-predator population (Fig. 5, C and D, tiger and wolf), and zooplankton communities in the Atlantic and the Indian Ocean, represented only by micro-zooplankton (Fig. 5, G and H). These predators are reported to be the dominant consumers of prey biomass in their respective ecosystems (14, 17, 22).

#### B. Conversion of raw data into standard units

Many of the meta-analyses that were combined for this study reported data in different units. Conversion into standard units required particular care, especially among aquatic systems, where mass variables may be reported in fresh or dry mass (picograms to tons) and density may be reported in areal or volumetric units. We avoided changing density dimensions (e.g., area to volume) in all but one case (one of four meta-analyses used in Fig. 5E), where the authors made clear how the data were estimated and provided mean lake depth, allowing conversion of mass per unit area into mass per unit volume (18).

Biomass density was converted to kg/km<sup>2</sup> for Figs. 1 and 3 and to g/m<sup>2</sup> or g/m<sup>3</sup> for Figs. 5 and 8. Changing units for all data in a plot in a consistent way has no effect on the scaling exponent but will alter the coefficient. However, the use of different conversion factors for different meta-analyses combined in the same plot can affect both the exponent and the coefficient. For example, each of Fig. 5, E, I, and J, combines multiple meta-analyses, some of which are reported in fresh mass, whereas others are in dry mass. We used conversion factors reported in the original studies to normalize data to a consistent set of units. Where conversion factors were not reported, we converted all dry mass or mass of carbon to fresh mass by multiplying by a factor of 10 (68). In these instances, we tested whether each meta-analysis yielded similar exponents in isolation; all of them were found to be within 0.1 of exponents from combined meta-analyses. Exponents reported in Fig. 5 are thus representative of the individual studies they comprise (table S2).

#### C. Methods for estimating biomass and production

Community biomass is the total mass density summed over all individuals in a given trophic level community (e.g., g/m<sup>2</sup>). Production is the total increase in biomass per unit time (e.g., g/m<sup>2</sup> per year), in the absence of consumption, which has the same units. Methods for estimating community biomass and production are not equivalent across ecosystem types, nor are they always equivalent across biomass gradients of similar species (Fig. 5). The same is true for body mass and individual production across the size spectrum (Fig. 6). Details of methods can be found in the original studies and summarized in the relevant places cited in database S1. A summary of methods for biomass and production measurements at the ecosystem level can be found in Cebrian and Lartigue (37) and at the individual level in Ernest *et al.* (71).

Despite attempts of different studies to estimate the same variables in standardized convertible units, combining data obtained through very different methods can cause inaccuracies in the scaling exponent. This is particularly true if there are any systematic biases across a biomass gradient. Many inaccuracies will likely be relatively small compared with the near two orders of magnitude over which many relations extend. Nonetheless, this was an important consideration for treating ecosystem types separately, where the most substantial divergences in methodology exist.

#### D. Regression method

Ordinary least squares (OLS) was used for all fits to log-transformed data, consistent with a number of other published cross-ecosystem meta-analyses (10, 19–21, 29–42). However, there is ongoing debate about which regression methods are least biased depending on the distribution of error between *x*- and *y*-axis variables (65, 89–96). OLS (type I) is the standard

approach in fitting bivariate power laws in biology (68, 95), but it assumes all error is in the  $y$  variable and thus tends to underestimate  $k$  as error in  $x$  increases. Type II regression methods, such as reduced major axis (RMA) and major axis (MA), partition error to both axes but can overestimate  $k$  as the error in  $y$  increases relative to  $x$  (65, 91, 93–96).

We assumed OLS to be the least biased slope estimator for the specific data that we report, given the greater fraction of error associated with  $y$ -axis variables compared with  $x$ -axis variables. Mammal predators, such as lion, hyena, tiger and wolf ( $y$  axis, Fig. 5, A to D), are considerably more difficult to census than their prey ( $x$  axis) because of their often nocturnal habits and relatively low densities, which cause greater potential for estimation error (14, 60, 97, 98). Top carnivores were also enumerated as single populations that are likely compensatory with other dominant guild members. The African savanna data shown in Fig. 1 are an exception because they estimate the entire community of large predators. Here, the exponent remains nearly unchanged from OLS ( $k = 0.73$ ) to MA ( $k = 0.75$ ) and RMA ( $k = 0.76$ ), but for individual lion and hyena to prey (Fig. 5, A and B), type II methods give exponents near  $k = 0.88$ . Similarly, zooplankton community biomass ( $y$  axis, Fig. 5, E to H) tends to be less well estimated than that of phytoplankton ( $x$  axis), because zooplankton aggregate and migrate in the water column (99). Estimating their biomass requires separate techniques for different components of the community [e.g., crustacean, rotifer, and protozoan (22, 100)], whereas phytoplankton measurements tend to converge on similar values (99, 101, 102). For the Atlantic and Indian Ocean (Fig. 5, G and H), macrozooplankton data were not available, and so the  $y$ -axis variable is also a partially incomplete community measure.

Error is thus likely greater in the  $y$  axis for predator-prey relations (Fig. 5, A to H), and the same is true for production-biomass relations (Fig. 5, I to P). As a dynamic variable, production has the additional dimension of time over standing stock biomass and should control or account for consumption and decomposition between time intervals (44). Moreover, production measurements often use a variety of techniques that can give significantly diverging values [grasslands (103), forests (104, 105), aquatic invertebrates (106)]. For data in Fig. 5, the majority of measurement error is in the  $y$ -axis variable, and therefore exponents derived from OLS are expected to provide the most robust predictions of the three regression approaches.

The precise distribution of error among axes remains difficult to ascertain. Reported  $k$  values likely underestimate the exponent, and all the more so as error increases. An RMA exponent can be estimated by dividing the OLS  $k$  value by the square root of the coefficient of determination ( $\sqrt{R^2}$ ) (65, 91). These statistics are listed in tables S1 to S5. The vast majority of analyzed data sets exhibit sublinear biomass scaling exponents under all three methods. Exponent val-

ues obtained by using RMA and MA are discussed further in section M3.

The relations shown here are bivariate, so that much of the statistical literature on power law fitting of univariate rank-frequency distributions may be less relevant (107, 108). Each axis variable was gathered independent of the other, often using different methodologies, and so there is no possibility that the strength of these patterns is due to indirectly regressing a variable against some proxy of itself (109).

## M2. African savanna data (Figs. 1 and 3)

The African savanna data set includes complete large mammal abundance estimates assembled across whole ecosystems. Most systems were censused over the entire extent of the protected area, which were only included in the database if all dominant large mammals (>5 kg) were counted. Data were checked against other published estimates, particularly for carnivore counts, where errors can most influence the fit (section M1D). On average, 22 species from a pool of 40 were estimated in each system, for a total of 1000 large mammal abundance estimates drawn from 190 published sources (Fig. 3A).

### A. African ecosystem attributes

The distribution of African protected areas span the savanna rainfall gradient, from Kalahari desert to Ngorongoro Crater (Fig. 9). The relationship of log rainfall to log herbivore biomass has been shown to yield significant slopes between  $k = 1.5$  and  $2.0$  (10, 110, 111). Our data include a large proportion of ecosystems where other sources of water dominate, which obscures the rainfall-to-herbivore relationship [Lake Manyara National Park (NP), Tarangire NP, the Okavango Delta, Amboseli NP, and the area around Sabie River in Kruger]. The 23 analyzed regions range in area from 100 to 40,000 km<sup>2</sup>, totaling more than 150,000 km<sup>2</sup>, over which census counts were made. Protected area map boundaries are from (112), and lion range from (113).

The relation of mammal abundance to body mass is highly variable across and within African protected areas (Fig. 3A). Mammal population density has previously been shown to scale with body mass by a negative exponent between  $k = -1$  to  $-1/2$  [also known as Damuth's law, or size-density scaling (5, 56, 68, 114)]. This size-density scaling relation extends over six orders of magnitude in body mass and also reveals that individuals of all size classes typically range in density over about three orders of magnitude. This high residual variation results in insignificant size-density correlations over a limited range in body size, as in Fig. 3A, even compensating for possible undercounting smaller animals [e.g., a factor of 10; page 91 of (115)].

Populations in Fig. 3A were aggregated into their respective ecosystems to study the size structure of each trophic community across different ecosystems. Mean body mass is described further below, in section M5. The histograms in Fig. 3B show the frequency of different size classes, averaged for the six systems with lowest and

highest prey biomass. The four herbivore size classes are 5 to 20, 20 to 50, 50 to 200, and 200 to 500 kg. The three carnivore size classes are the three smallest carnivores combined (wild dog, leopard, and cheetah; 20 to 40 kg), hyena (50 kg), and lion (125 kg). The slight change in some herbivore size classes is small relative to the changes in trophic structure shown in Figs. 1 and 3C.

The predator-prey biomass scaling pattern shown in Fig. 1 and their ratio in Fig. 3C includes the five dominant African carnivores (lion, spotted hyena, leopard, cheetah, and wild dog), which compete for prey ranging from 5 to 500 kg (50, 51). In the Savuti region of Chobe NP, mega-herbivores (>750 kg) are frequently preyed upon by lions in the dry season (116) and were included as prey in this ecosystem (Fig. 9). We excluded the migrant population biomass of wildebeest, zebra, and gazelle in regions such as the Serengeti ecosystem and Masai Mara GR, which are known to largely escape predators, but nonetheless provide important prey subsidies to carnivores (117). Excluding migrant biomass, Serengeti and Masai Mara become the largest outliers above the best fit line (Fig. 9), possibly because of the exclusion of these subsidies. The largest outlier below the line is in Katavi NP (Fig. 9), where previous research has also reported relatively few predators (118).

### B. Robustness of the African predator-prey pattern

The African predator-prey pattern appears to be robust to the following: (i) how ecosystems are replicated at different time periods, (ii) what species are included in predator and prey communities, (iii) variations in species body mass, (iv) possible systematic bias in sampling, and (v) alternative regression approaches. These considerations are elaborated further below.

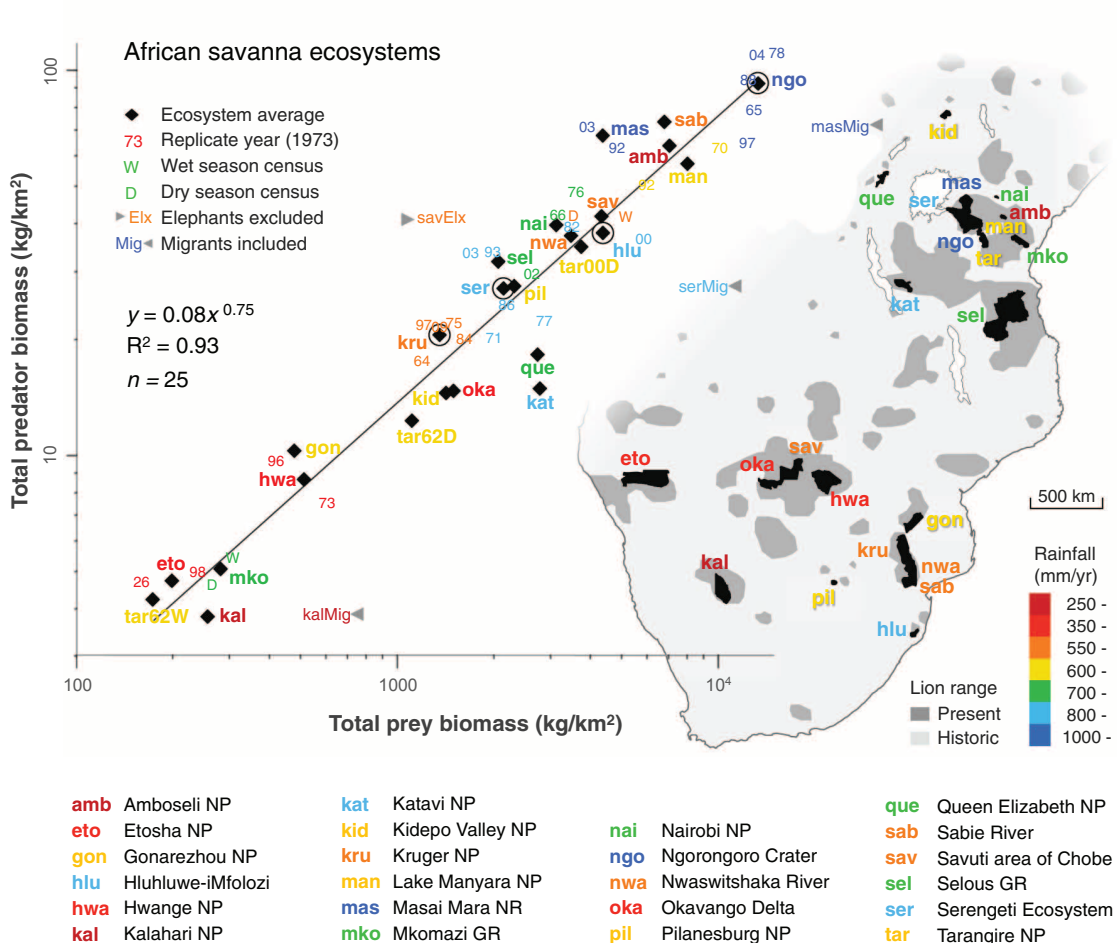
1) Predator and prey biomass were fit to 23 protected areas, some of which were sampled in different decades for a total of  $n = 46$  ecosystem time periods. Replicate time periods are averaged in Fig. 9 (and Fig. 10A) to give equal weighting to each area. Tarangire NP is the only system not averaged given large biomass fluctuations between wet and dry seasons in 1962 and 2000. The resultant fit is very similar to Fig. 1 ( $k = 0.75$ ;  $n = 25$  protected ecosystems  $R^2 = 0.93$ ), suggesting there are no biases from possible pseudo-replication.

2) The pattern holds under alternative assumptions about the breadth of the prey community. We excluded mega-herbivores from the prey community, although carnivores will consume juveniles and carcasses of mega-herbivores, such as giraffe and elephant. Including mega-herbivores as prey in all ecosystems slightly reduces the exponent and goodness of fit but is otherwise quite similar ( $k = 0.66$ ;  $R^2 = 0.65$ ; Fig. 10C).

3) The pattern is robust to variations in species body mass. Given that community composition is largely invariant across the prey biomass gradient (Fig. 3B), the sublinear scaling evident between total predator and prey biomass is also evident for numerical density (Fig. 10B;  $k = 0.63$ ;  $R^2 = 0.86$ ) and implies that the pattern is largely robust to

**Fig. 9. African savanna ecosystem characteristics.** These data are shown in Fig. 1, but here abundance in different time periods are averaged to give equal weight to each protected area ( $k = 0.75$ ; 95% CI = 0.66, 0.83;  $n = 23$ ). We excluded migrant biomass in Serengeti and Masai Mara, which include the largest three outliers above the line (ser and mas). Mega-herbivores were excluded as prey in all but the Savuti region of Chobe NP (sav), where lions prey on elephants (116). When excluded from Savuti, the point becomes a notable outlier (savElx). The largest outlier below the line is Katavi NP (kat), where previous research has reported relatively few predators (118). Tarangire (tar) is not averaged due to large biomass fluctuations.

Black circles are the ecosystems in which time series data are shown in Fig. 10D.



assumptions about species body mass. Systematic changes in average species body mass exhibited by some mammals across ecosystems are never more than a factor of two and thus not sufficient to account for these sublinear scaling patterns.

4) Although it is possible that there are systematic biases of sampling one or both trophic groups at high or low densities, this seems unlikely. The linear prediction of Carbone and Gittleman (53) is shown by the dotted line in Fig. 1 and Fig. 3C, which predicts that 111 kg of prey are needed for every 1 kg of predator. The ecosystems that most distinguish the predator-prey scaling relation from this prediction lie at the far left of the regression. Among these, five whole-ecosystem censuses of all predators and prey were estimated by the same authors: Hwange (119), Mkomazi wet and dry season (120), Tarangire wet season (121), and Kalahari (122). This suggests that similar censusing methods were applied to both predators and prey communities and that the deviation from a linear prediction is unlikely a result of bias. More generally, at least four independent meta-analyses of a similar nature have been conducted across African ecosystems, all of which yield similar sublinear patterns (9–12) ( $k$  ranges 0.67 to 0.80; Fig. 11A and table S2.1–4).

5) Last, the scaling pattern is robust to alternative regression methods such as type II, which

yield exponents well within the confidence interval (CI) of the least squares fit (95% CI = 0.66 to 0.79; major axis  $k = 0.75$  and reduced major axis  $k = 0.76$ ; see section M1D).

### C. Population compensation in space and time

African mammal populations appear to be compensatory in space and time, which allows greater regularity to emerge among whole communities than among individual populations. For example, the community-level predator-prey pattern shown in Fig. 1 is not evident because fewer species are aggregated into the community. Although the relations of lion and hyena to total prey biomass give robust scaling patterns, they exhibit greater dispersion (Fig. 5A,  $R^2 = 0.77$ , and Fig. 5B,  $R^2 = 0.69$ ) than the whole predator community pattern (Fig. 1,  $R^2 = 0.92$ ). In ecosystems where lion are above the line, hyena tend to be below, and vice versa (Fig. 5, A and B). Given this compensation among predator populations, higher  $R^2$  is obtained when lion and hyena are summed together and highest by further aggregating the large carnivore biomass of leopard, cheetah, and wild dog populations, all of which compete for similar prey (50, 51).

Prey populations are also compensatory relative to predators. When fewer populations are included in the prey community, the predator-

prey pattern exhibits greater dispersion, so that even dominant populations, such as lion versus zebra or hyena versus impala, exhibit little or no pattern (all  $R^2 < 0.4$  for population-level predator-prey relations). Prey also exhibit compensation within any given ecosystem in time. Population biomass time series for lion and the six most dominant African prey species were assembled across four large protected areas (Kruger NP, Hluhluwe-iMfolozi NP, Serengeti ecosystem, and Ngorongoro Crater; Fig. 10D). In nearly all cases the coefficient of variation (standard deviation divided by mean) is lower, indicating less fluctuation, for total prey community biomass than it is for the populations it comprises. This implies that populations are compensatory in time (Fig. 10D), which is consistent with the emergence of the predator-prey pattern at the ecosystem-level.

### M3. Global community data (Fig. 5)

Community-level data aggregate many thousands of population counts across 2260 ecosystems globally and are drawn from over 850 published sources, some of which include meta-analyses of additional studies. Units were converted to g/m<sup>2</sup> for all terrestrial biomass data (Fig. 5, A to D and I to L). Aquatic predator-prey data (Fig. 5, E to H) were originally reported in various volumetric units and converted to g/m<sup>3</sup>. All production-biomass data, including aquatic studies (Fig. 5, I

**Fig. 10. African mammal biomass, numerical density relations, and population time series.**

(A) This relation duplicates Fig. 9 (colored according to rainfall) to allow comparisons to the pyramid of numbers (B) and prey biomass including mega-herbivores (C). Note that Savuti is excluded and Tarangire is not averaged for reasons outlined in Fig. 9. (B) Predator-prey total numerical density shows a similar pattern because of the near invariance of mean body mass with community biomass (Fig. 3B). The lower exponent is driven largely by two areas of Kruger NP (sab and nwa; orange triangles) with high densities of impala. The exponent for all ecosystem time periods, omitting sab and nwa, is  $k = 0.70$  ( $n = 42$ ;  $R^2 = 0.90$ ).

(C) Predator to total herbivore biomass, including all the prey in (A) plus all mega-herbivores (giraffe to elephant). The exponent for all ecosystem-time periods is  $k = 0.70$  ( $n = 44$ ;  $R^2 = 0.67$ ).

(D) Population biomass time series for dominant species in each of four protected areas with complete ecosystem censuses. Replicate years used in Fig. 1 are labeled in color and chosen on the basis of available census data for all species. Total prey biomass has a consistently lower coefficient of variation (standard deviation divided by mean; CV) than the population biomass it comprises for all but two populations in Serengeti (ser), where data are sparse. The CV for total prey biomass is as follows (with min. and max. CV for the six dominant herbivore populations): kru—0.196 (0.20, 0.40); hlu—0.29 (0.32, 0.69); ser—0.30 (0.20, 0.53); ngo—0.16 (0.19, 0.73).

to P), were originally reported in areal units and converted to  $\text{g/m}^2$  (section M1B). The principal meta-analyses contributing to the data in Fig. 5 are summarized in Fig. 11 and tables S1 and S2.

We used OLS for all fits to data, which are believed to provide the least biased predictions of available methods (see section M1D). We considered two alternative regression methods to fit the data in Fig. 5, using the ‘smatr’ library package in R (123): RMA and MA. Excluding fish (Fig. 5P) for the reasons stated in section M3P, type II regression approaches (RMA and MA) yield sublinear exponents for all plots in Fig. 5, except where data are highly dispersed ( $R^2 < 0.5$ ,  $k$  near 1; Fig. 5, F, G and L). The same is also true for published cross-system meta-analyses summarized in Fig. 11 and table S2.

#### Predator-prey scaling (Fig. 5 A to H) A and B. Lion and hyena to prey

Data are shown aggregated with other predators in Figs. 1 and 3 (see also Fig. 9). These data derive from 190 publications and are described further in section M2. Four meta-analyses reveal sublinear scaling in isolation [Farlow (9), East (10), Hemson (11), and Grange and Duncan

(12);  $k$  ranges 0.66 to 0.80; Fig. 11A and table S2.1-4]

#### C. Tiger to prey

Data are from averages of 829 large mammal population censuses in India from Project Tiger combined with 22 other studies undertaken throughout Southeast Asia. Three of these studies are large-scale meta-analyses that each reveals sublinear scaling in isolation [Project Tiger (13), Karanth *et al.* (14), and Kawanishi and Sunquist (15);  $k$  ranges 0.62 to 0.79; Fig. 11B and table S2.5-7].

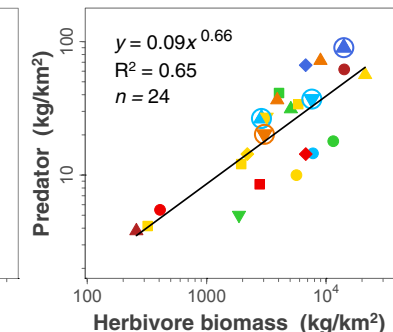
#### D. Wolf to prey

Data are from two meta-analyses: Fuller (16) and Messier (17). Messier lists only moose as prey, claiming they represent at least 75% of all prey in the ecosystems studied. Six sites with reported heavy wolf exploitation were removed. Both studies alone each reveal sublinear scaling ( $k$  ranges 0.72 to 0.87; Fig. 11C; table S2.8-9).

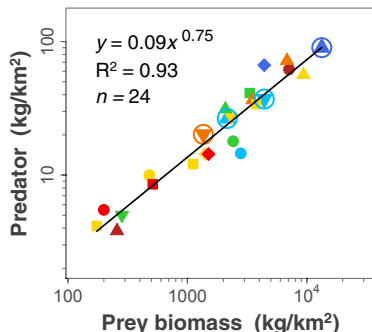
#### E. Freshwater zooplankton to algae

Data are from four meta-analyses: Cyr and Peters (18) (average estimates from the International Biological Program, converted from areal to volu-

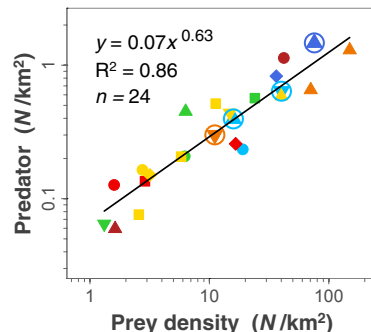
#### C Including megaherbivores



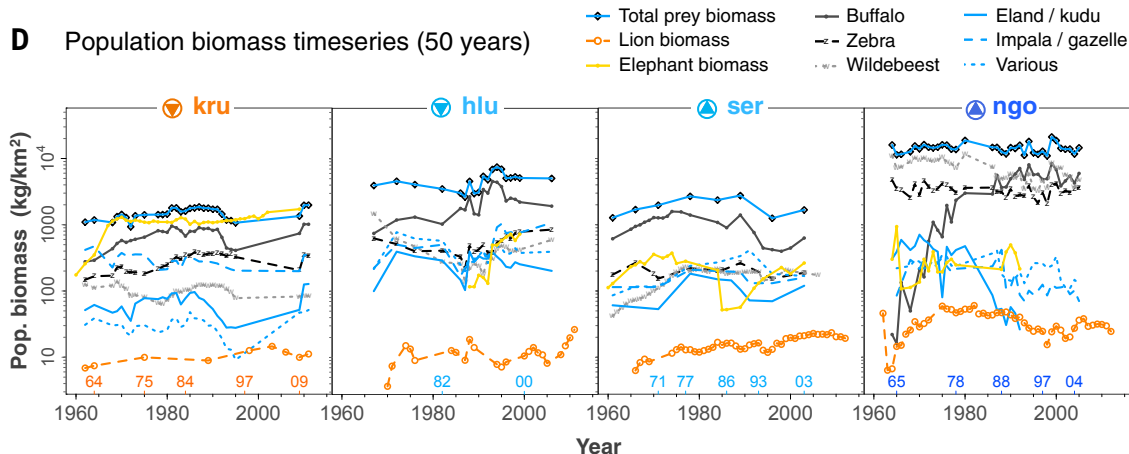
#### A Predator-prey biomass



#### B Numerical density



#### D Population biomass timeseries (50 years)



metric units on the basis of reported mean lake depth); McCauley and Kalff (19) (averages of 207 plankton community estimates); del Giorgio and Gasol (20); and del Giorgio *et al.* (21). All studies reveal sublinear scaling in isolation ( $k$  ranges 0.64 to 0.72; Fig. 11, D and E, and table S2.10-14).

#### F to H. Marine zooplankton to algae

Data are from Irigoien *et al.* (22). English Channel (F) data include multiple stations at various time periods, which estimate total zooplankton and phytoplankton community biomass. Atlantic (G) and Indian (H) ocean data include only microzooplankton, which the authors claim are the main consumers of algae in oceans. One extreme Atlantic point is removed ( $k = 0.67$  with point included). When all microzooplankton to algae are combined across Atlantic, Indian, and a number of other marine areas ( $n = 547$ ), the exponent  $k$  equals 0.54 (Fig. 11F and table S2.15).

#### Production-biomass scaling (Fig. 5, I to P) I. and J. Grassland P-B

Data are from six meta-analyses from the International Biological Program, notably Coupland (23), Sims *et al.* (24), and Sims and Singh (25).

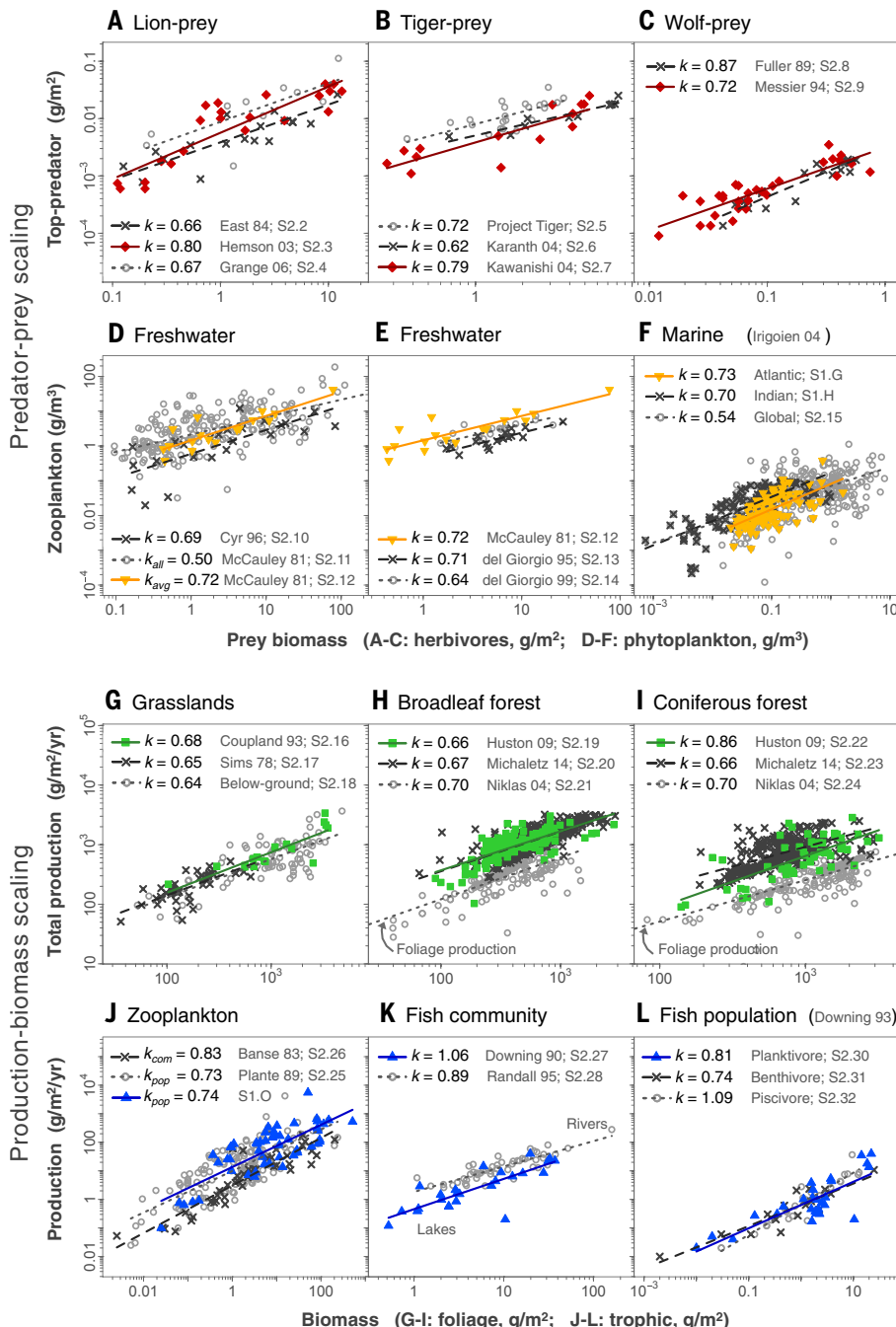


**Fig. 11. Published cross-system meta-analyses contributing to regressions in Fig. 5. (A to L)** These plots each derive from a single source and show similar scaling to combined plots in Fig. 5 (table S2).

These three studies yield sublinear scaling in isolation for both total and above-ground *P-B* [(23–25);  $k$  ranges 0.64 to 0.68; Fig. 11G and table S2.16–18].

#### K and L. Forest *P-B*

Total production to foliage biomass data are from two large meta-analyses: Huston and Wolverton (26), which includes global data digitized from Cannell (27), and Michaletz *et al.* (28), with sites mostly in China, most of which

derive from Luo (124), described in Ni *et al.* (125). Foliage biomass (*x* axis) excludes all stem, branch, and root material, representing the most photosynthetically active biomass, whereas total production includes all forest growth. Similar exponent values are obtained for foliage production to foliage biomass from the Niklas and Enquist data set (66), which is also from Cannell (27). We removed all sites with reported growing seasons less than 6 months in order to better compare annual production across sites. Relaxing

this assumption has no effect on exponent values for forests from Cannell (27) but lowers exponents for needleleaf sites from Michaletz *et al.* (28). One extreme point was removed from each of broadleaf and coniferous forests, as noted in the data set. All three studies reveal sublinear scaling in isolation [(26, 28, 66);  $k$  ranges 0.66 to 0.86; Fig. 11, H to I, and table S2.19–24].

#### M. Seagrass bed *P-B*

Data were digitized from Duarte and Chiscano (29), authors' figure 2. Original data and geo-coordinates are not available. These data are not mapped in Fig. 5 and are excluded from Fig. 7. Original statistics are reproduced from authors' page 170.

#### N. Algae *P-B*

Data from International Biological Program were compiled and averaged in Cyr and Peters (18). These data are for 24 of the same lakes as in Fig. 5E, providing one of the few direct comparisons between predator-prey and production-biomass scaling across the same ecosystems.

#### O. Zooplankton *P-B*

Data were from Plante and Downing (30). These data were originally reported at the population level but were aggregated into community measures in Fig. 5O. The authors reported a similar production-biomass exponent at the population level ( $k = 0.73$ ;  $n = 164$  populations; table S2.25). A somewhat higher exponent ( $k = 0.83$ ;  $n = 43$  populations) is reported for invertebrate population production-biomass by Banse and Mosher (67) (Fig. 11J and table S2.26).

#### P. Fish *P-B*

Data from two meta-analyses of Downing and Plante [(31); lakes;  $n = 25$ ] and Randall [(32); rivers;  $n = 51$ ]. Each study reveals similar scaling in isolation ( $k$  ranges 0.89 to 1.06; Fig. 11K and table S2.27–28). The fish community is composed of multiple trophic groups, and it is possible that lower trophic levels exhibit sublinear scaling. The meta-analysis of Downing and Plante (33) is at the population level for lake fish and shows that benthivores and planktivores scale as  $k = 0.74$  and  $k = 0.81$ , whereas piscivores scale as  $k = 1.09$  (Fig. 11L and table S2.29–32). The near-linear ( $k = 1$ ) scaling of the higher level piscivores may be dominating the whole fish community relation shown in Fig. 5P.

#### Flux of primary production (Fig. 12)

##### Q. Consumption and primary production

In both terrestrial and aquatic systems globally, herbivore consumption and decomposition have been shown to scale near linearly ( $k$  near 1) with primary production (36, 37). This suggests that there are no systematic changes in the proportion of primary production transferred to herbivores or decomposers as production increases. Data from these meta-analyses are reproduced in Fig. 12; regressions are summarized in table S5 and are broadly similar to the original analyses by Cebran (36, 37). Scaling exponents tend to

range from near  $k = 0.9$  to just above 1 for consumption ( $n = 247$ ) and near 1 or slightly above for decomposition ( $n = 232$  ecosystems). However, terrestrial herbivore biomass to primary production tends to be closer to  $k = 1.2$  or 1.3, which is not fully understood and is hindered by data limitations. Linear consumption and decomposition scaling with primary production is consistent with the link between trophic structure and production. It implies a general steady state, whereby production into the plant community is matched by similar ratios of consumption out of the community.

#### M4. Individual production data (Figs. 6 and 7)

At the individual level, a great variety of vital rates scale with body mass near  $k = \frac{3}{4}$  (5, 68). Individual maximum whole-organism annual production to adult body mass is notable for exhibiting  $k = \frac{3}{4}$  across all eukaryotes without large discrete shifts between major taxa, as there are, for example, among metabolic allometries across this same size spectrum (69, 126). Whole-organism production is measured differently for different species but seeks to estimate the total biomass added in a standard unit of time that can be attributed to a single individual. This combines both somatic and reproductive growth, as detailed in Ernest *et al.* (71) for different taxa. Figure 6 excludes prokaryotes and birds, because these taxa are not represented at the ecosystem level in Fig. 5.

The individual production allometry ( $n = 1635$  estimates from 1098 species) derives from 362 published sources and principally from the following meta-analyses: multiple taxa—Ernest *et al.* (71) and Savage *et al.* (127); mammals—Duncan *et al.* (128), Fagan *et al.* (129), and Pereira and Daily (130); protists—DeLong *et al.* (77); land plants—Niklas and Enquist (66), after Cannell (27); ectotherms—Plante and Downing (30), invertebrates, and Downing and Plante (31); fish.

Regressions of the full data set ( $n = 1705$  estimates; 1283 species spanning 146 taxonomic orders and 276 families) reveal equivalent scaling across 21 orders of magnitude (table S3.1-3). Regression statistics at more detailed taxonomic resolution are shown in table S3. Bacteria appear to have steeper scaling ( $k > 1$ ) than other taxa (77). Note that exponents for prokaryotes and protists are OLS derived and thus differ from RMA-derived slopes reported in DeLong *et al.* (77).

Figure 7 compares production-mass exponents at the ecosystem level (Fig. 5) with the individual level (Fig. 6). Ecosystem-level exponents were obtained by fitting a single slope and multiple categorical variables (one for each plot) to the relevant data in Fig. 5. Each colored taxonomic group for the individual data in Fig. 6 was fit to a single slope. Data at the ecosystem level (Fig. 5) and individual level (Fig. 6) are as follows: mammal—Fig. 5, A to D ( $n = 184$  data points) and Fig. 6 in red ( $n = 1061$ ); protist—Fig. 5, E to H and N ( $n = 691$ ) and Fig. 6 in yellow ( $n = 137$ ); plant—Fig. 5, I to L ( $n = 1153$ ) and Fig. 6 in green ( $n = 132$ ); ectotherm—Fig. 5, O and P ( $n = 127$ ) and Fig. 6 in blue ( $n = 305$ ). Seagrass beds (Fig. 5M) were excluded from the comparison because the original data are not available (section M3M) and no data for individual seagrass production and plant mass are available. We repeated this comparison only with plots with  $R^2 > 0.5$  (thus excluding Fig. 5, F, G, and L) and found no discernible difference to the scaling exponents or confidence intervals. More detailed comparison can be made from tables S1 to S3.

#### M5. Mean body mass data (Fig. 8)

Community data from Fig. 5 were decomposed into population-level values to calculate mean body mass ( $b$ ) plotted against community biomass ( $B$ ). The plots in Fig. 8 combine ecosystems from multiple plots in Fig. 5, A to D, F to

H, K to L, and O and P. Similar poor correlations between these variables are observed for distinct ecosystem types, as shown by detailed regressions in table S4. No individual size data were available for grasslands or seagrass beds (Fig. 5, I, J, and M), and so these community types are not included in Fig. 8. Mean body mass is the sum of the abundance ( $N$ ) of each species ( $j$ ) in a trophic community multiplied by the unit body mass for the population ( $b_j$ ) and divided by the sum of all organisms in the ecosystem. This is equivalent to total biomass divided by total numerical density for a trophic community.

$$\bar{b} = \frac{\sum N_j b_j}{\sum N_j}$$

#### A. Large mammal carnivores

Mean body mass to carnivore community biomass combines systems from Africa (lion, spotted, hyena, leopard, cheetah, and wild dog) and Asia [tiger, leopard, striped hyena, wolf, and dhole; from Project Tiger (13)]. Carnivore mean body mass tends to be higher in Asia than in Africa because of the larger-bodied tigers (table S4.3-5). This plot includes data shown in Fig. 3B. Note that in Fig. 3B, African mean carnivore size is plotted against herbivore prey biomass, whereas in Fig. 8A it is plotted against carnivore biomass (and combined with Indian carnivores).

#### B. Large mammal herbivores

Mean body mass to herbivore biomass data combines all the African, Asian, and North American ecosystems in Fig. 5, A to D (table S4.2, 6-7). This plot includes data shown in Fig. 3B.

#### C. Broadleaf and coniferous forest

Body mass includes all wood, branch, and foliage mass per tree, whereas biomass includes only foliage biomass per unit area (as in Fig. 5, K and L). Mean tree size to foliage biomass combines data in Fig. 5, K and L, from Huston and Wolverton (26), digitized from Cannell (27). The number of stems per site was not available in Michaletz *et al.* (28), and so sites in China are not included. The lack of any systematic size structure relation is also evident in the Niklas and Enquist data set (27, 66). These regressions tend to be influenced by a few extreme points, but most are not significant with low  $R^2$  values. (table S4.8-13).

#### D. Fish

Mean body mass to biomass is for the same ecosystems as shown in Fig. 5P {Downing *et al.* [lakes (31)] and Randall [rivers (32)]}. The slightly negative relation is due to the combination of lake and river fish, the former of which has larger mean size and lower community biomass. None of these relations in isolation is significant (table S4.14-16).

#### E. Lake zooplankton ( $\text{g}/\text{m}^3$ )

Digitized from Cyr and Pace (52), combining authors' figure 4, A and B, each of which are

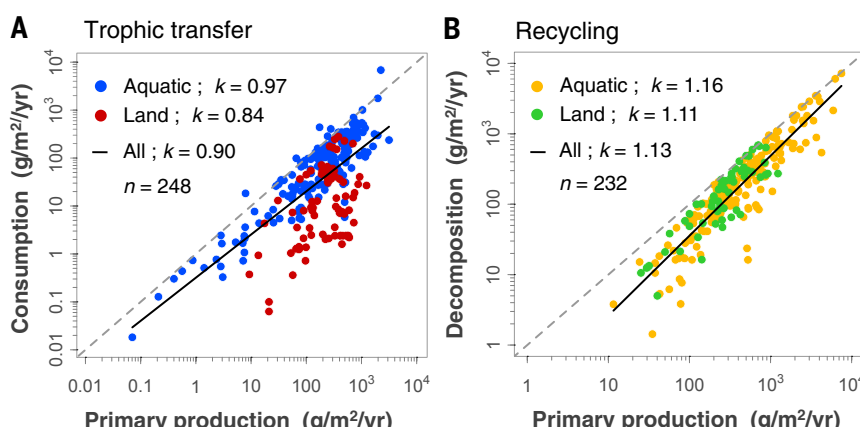


**Fig. 12. A near-constant fraction of primary production is transferred to herbivores and decomposers.** Data show near-linear ( $k = 1$ ) scaling in the fraction of primary production (A) transferred to herbivore consumption and (B) recycled to decomposers, across global productivity gradients. This suggests few systematic changes in the ratios of flux rates. These data and regressions are reported in Cebrian and Cebrian and Lartigue (36, 37), combining 196 original published sources. Further details are available in the original studies (36, 37) and table S5.

also significant relations with exponents ranging from  $k = 0.26$  to  $0.41$ . These ecosystems are not the same as shown in Fig. 5, E or O, although there is likely overlap for lakes in Québec. Data were originally presented as zooplankton biomass on the  $y$  axis and mean body mass on the  $x$  axis, which are reversed in Fig. 8E (table S4.17–19). The data shown in Fig. 8E are approximate.

### F. Marine algae ( $\text{g}/\text{m}^3$ )

Digitized from Irigoien *et al.* (22), authors' figure 3a. Mean algal cell size to biomass data are for the English Channel, the Atlantic, and the Indian Ocean (Fig. 5, F to H; table S4.20–24). The authors reported  $k = 0.44$  for their global data set, which includes numerous additional sites. The data shown in Fig. 8F are approximate.

### REFERENCES AND NOTES

- S. A. Frank, The common patterns of nature. *J. Evol. Biol.* **22**, 1563–1585 (2009). doi: [10.1111/j.1420-9101.2009.01775.x](https://doi.org/10.1111/j.1420-9101.2009.01775.x); pmid: [19538344](https://pubmed.ncbi.nlm.nih.gov/19538344/)
- P. A. Marquet *et al.*, Scaling and power-laws in ecological systems. *J. Exp. Biol.* **208**, 1749–1769 (2005). doi: [10.1242/jeb.01588](https://doi.org/10.1242/jeb.01588); pmid: [15855405](https://pubmed.ncbi.nlm.nih.gov/15855405/)
- J. H. Brown, B. A. Maurer, Macroecology: The division of food and space among species on continents. *Science* **243**, 1145–1150 (1989). doi: [10.1126/science.243.4895.1145](https://doi.org/10.1126/science.243.4895.1145); pmid: [17799895](https://pubmed.ncbi.nlm.nih.gov/17799895/)
- S. A. Levin, The problem of pattern and scale in ecology: The Robert H. MacArthur award lecture. *Ecology* **73**, 1943–1967 (1992). doi: [10.2307/1941447](https://doi.org/10.2307/1941447)
- J. H. Brown, J. F. Gillooly, A. P. Allen, V. M. Savage, G. B. West, Toward a metabolic theory of ecology. *Ecology* **85**, 1771–1789 (2004). doi: [10.1890/03-9000](https://doi.org/10.1890/03-9000)
- R. M. Sibly, J. H. Brown, A. Kodric-Brown, *Metabolic Ecology: A Scaling Approach* (Wiley, New York, 2012).
- J. Harte, *Maximum Entropy and Ecology: A Theory of Abundance, Distribution, and Energetics* (Oxford Univ. Press, Oxford, 2011).
- M. Loreau, *From Populations to Ecosystems: Theoretical Foundations for a New Ecological Synthesis (MPB-46)* (Princeton Univ. Press, Princeton, NJ, 2010).
- J. O. Farlow, A consideration of the trophic dynamics of a Late Cretaceous large-dinosaur community (Oldman Formation). *Ecology* **57**, 841–857 (1976). doi: [10.2307/1941052](https://doi.org/10.2307/1941052)
- R. East, Rainfall, soil nutrient status and biomass of large African savanna mammals. *Afr. J. Ecol.* **22**, 245–270 (1984). doi: [10.1111/j.1365-2028.1984.tb00700.x](https://doi.org/10.1111/j.1365-2028.1984.tb00700.x)
- G. Hemson, thesis, University of Oxford, Oxford, UK (2003).
- S. Grange, P. Duncan, Bottom-up and top-down processes in African ungulate communities: Resources and predation acting on the relative abundance of zebra and grazing bovids. *Ecohydrology* **29**, 899–907 (2006). doi: [10.1111/j.2006.0906-7590.04684.x](https://doi.org/10.1111/j.2006.0906-7590.04684.x)
- Project Tiger Directorate, Reserve Guide: Project Tiger Reserves in India. *Project Tiger India*, [projecttiger.nic.in/map.htm](http://projecttiger.nic.in/map.htm).
- K. U. Karanth, J. D. Nichols, N. S. Kumar, W. A. Link, J. E. Hines, Tigers and their prey: Predicting carnivore densities from prey abundance. *Proc. Natl. Acad. Sci. U.S.A.* **101**, 4854–4858 (2004). doi: [10.1073/pnas.0306210101](https://doi.org/10.1073/pnas.0306210101); pmid: [15041746](https://pubmed.ncbi.nlm.nih.gov/15041746/)
- K. Kawanishi, M. E. Sunquist, Conservation status of tigers in a primary rainforest of Peninsular Malaysia. *Biol. Conserv.* **120**, 329–344 (2004). doi: [10.1016/j.biocon.2004.03.005](https://doi.org/10.1016/j.biocon.2004.03.005)
- T. K. Fuller, Population dynamics of wolves in North-Central Minnesota. *Wildl. Monogr.* **105**, 1–41 (1989).
- F. Messier, Ungulate population models with predation: A case study with the North American moose. *Ecology* **75**, 478–488 (1994). doi: [10.2307/1939551](https://doi.org/10.2307/1939551)
- H. Cyr, R. H. Peters, Biomass-size spectra and the prediction of fish biomass in lakes. *Can. J. Fish. Aquat. Sci.* **53**, 994–1006 (1996). doi: [10.1139/f96-033](https://doi.org/10.1139/f96-033)
- E. McCauley, J. Kalf, Empirical relationships between phytoplankton and zooplankton biomass in lakes. *Can. J. Fish. Aquat. Sci.* **38**, 458–463 (1981). doi: [10.1139/f81-063](https://doi.org/10.1139/f81-063)
- P. A. del Giorgio, J. M. Gasol, Biomass distribution in freshwater plankton communities. *Am. Nat.* **146**, 135–152 (1995). doi: [10.1086/285790](https://doi.org/10.1086/285790)
- P. A. del Giorgio, J. J. Cole, N. F. Caraco, R. H. Peters, Linking planktonic biomass and metabolism to net gas fluxes in northern temperate lakes. *Ecology* **80**, 1422–1431 (1999). doi: [10.1890/0012-9658\(1999\)080\[1422:LBAMT\]2.0.CO;2](https://doi.org/10.1890/0012-9658(1999)080[1422:LBAMT]2.0.CO;2)
- X. Irigoien, J. Huisman, R. P. Harris, Global biodiversity patterns of marine phytoplankton and zooplankton. *Nature* **429**, 863–867 (2004). doi: [10.1038/nature02593](https://doi.org/10.1038/nature02593); pmid: [15215862](https://pubmed.ncbi.nlm.nih.gov/15215862/)
- R. T. Coupland, *Natural Grasslands: Eastern Hemisphere and Résumé* (Elsevier, Amsterdam, ed. 1, 1993), vol. 8B.
- P. L. Sims, J. S. Singh, W. K. Lauenroth, The structure and function of ten Western North American grasslands: I. Abiotic and vegetational characteristics. *J. Ecol.* **66**, 251–285 (1978). doi: [10.2307/2259192](https://doi.org/10.2307/2259192)
- P. L. Sims, J. S. Singh, The structure and function of ten Western North American grasslands: III. Net primary production, turnover and efficiencies of energy capture and water use. *J. Ecol.* **66**, 573–597 (1978). doi: [10.2307/2259152](https://doi.org/10.2307/2259152)
- M. A. Huston, S. Wolverton, The global distribution of net primary production: Resolving the paradox. *Ecol. Monogr.* **79**, 343–377 (2009). doi: [10.1890/08-0588.1](https://doi.org/10.1890/08-0588.1)
- M. G. R. Cannell, *World Forest Biomass and Primary Production Data* (Academic Press, London, 1982).
- S. T. Michaletz, D. Cheng, A. J. Kerkhoff, B. J. Enquist, Convergence of terrestrial plant production across global climate gradients. *Nature* **512**, 39–43 (2014). pmid: [25043056](https://pubmed.ncbi.nlm.nih.gov/25043056/)
- C. M. Duarte, C. L. Chiscano, Seagrass biomass and production: A reassessment. *Aquat. Bot.* **65**, 159–174 (1999). doi: [10.1016/S0304-3770\(99\)00038-8](https://doi.org/10.1016/S0304-3770(99)00038-8)
- C. Plante, J. A. Downing, Production of freshwater invertebrate populations in lakes. *Can. J. Fish. Aquat. Sci.* **46**, 1489–1498 (1989). doi: [10.1139/f89-191](https://doi.org/10.1139/f89-191)
- J. A. Downing, C. Plante, S. Lalonde, Fish production correlated with primary productivity, not the morphoedaphic index. *Can. J. Fish. Aquat. Sci.* **47**, 1929–1936 (1990). doi: [10.1139/190-217](https://doi.org/10.1139/190-217)
- R. G. Randall, C. K. Minns, J. R. M. Kelso, Fish production in freshwater: Are rivers more productive than lakes? *Can. J. Fish. Aquat. Sci.* **52**, 631–643 (1995). doi: [10.1139/f95-063](https://doi.org/10.1139/f95-063)
- J. A. Downing, C. Plante, Production of fish populations in lakes. *Can. J. Fish. Aquat. Sci.* **50**, 110–120 (1993). doi: [10.1139/f93-013](https://doi.org/10.1139/f93-013)
- S. J. McNaughton, M. Oesterheld, D. A. Frank, K. J. Williams, Ecosystem-level patterns of primary productivity and herbivory in terrestrial habitats. *Nature* **341**, 142–144 (1989). doi: [10.1038/341142a0](https://doi.org/10.1038/341142a0); pmid: [2779651](https://pubmed.ncbi.nlm.nih.gov/2779651/)
- H. Cyr, M. L. Pace, Magnitude and patterns of herbivory in aquatic and terrestrial ecosystems. *Nature* **361**, 148–150 (1993). doi: [10.1038/361148a0](https://doi.org/10.1038/361148a0)
- J. Cebrán, Patterns of the fate of production in plant communities. *Am. Nat.* **154**, 449–468 (1999). doi: [10.1086/303244](https://doi.org/10.1086/303244); pmid: [10523491](https://pubmed.ncbi.nlm.nih.gov/10523491/)
- J. Cebrán, J. Lartigue, Patterns of herbivory and decomposition in aquatic and terrestrial ecosystems. *Ecol. Monogr.* **74**, 237–259 (2004). doi: [10.1890/03-4019](https://doi.org/10.1890/03-4019)
- J. M. Gasol, P. A. del Giorgio, C. M. Duarte, Biomass distribution in marine planktonic communities. *Limnol. Oceanogr.* **42**, 1353–1363 (1997). doi: [10.4319/lo.1997.42.6.1353](https://doi.org/10.4319/lo.1997.42.6.1353)
- J. Cebrán, C. M. Duarte, The dependence of herbivory on growth rate in natural plant communities. *Funct. Ecol.* **8**, 518–525 (1994). doi: [10.2307/2390077](https://doi.org/10.2307/2390077)
- J. Cebrán *et al.*, Producer nutritional quality controls ecosystem trophic structure. *PLOS ONE* **4**, e4929 (2009). pmid: [19300514](https://pubmed.ncbi.nlm.nih.gov/19300514/)
- M. A. Leibold, J. M. Chase, J. B. Shurin, A. L. Downing, Species turnover and the regulation of trophic structure. *Annu. Rev. Ecol. Syst.* **28**, 467–494 (1997). doi: [10.1146/annurev.ecolsys.28.1.467](https://doi.org/10.1146/annurev.ecolsys.28.1.467)
- J. M. Chase, M. A. Leibold, A. L. Downing, J. B. Shurin, The effects of productivity, herbivory, and plant species turnover in grassland food webs. *Ecology* **81**, 2485–2497 (2000). doi: [10.1890/0012-9658\(2000\)081\[2485:TEOPHA\]2.0.CO;2](https://doi.org/10.1890/0012-9658(2000)081[2485:TEOPHA]2.0.CO;2)
- C. S. Elton, *Animal Ecology* (Univ. of Chicago Press, Chicago, IL, 1927).
- E. P. Odum, *Fundamentals of Ecology* (Saunders, Philadelphia, ed. 3, 1971).
- R. Trebilco, J. K. Baum, A. K. Salomon, N. K. Dulvy, Ecosystem ecology: Size-based constraints on the pyramids of life. *Trends Ecol. Evol.* **28**, 423–431 (2013). doi: [10.1016/j.tree.2013.03.008](https://doi.org/10.1016/j.tree.2013.03.008); pmid: [23623003](https://pubmed.ncbi.nlm.nih.gov/23623003/)
- M. L. Rosenzweig, Paradox of enrichment: Destabilization of exploitation ecosystems in ecological time. *Science* **171**, 385–387 (1971). doi: [10.1126/science.171.3969.385](https://doi.org/10.1126/science.171.3969.385); pmid: [5538935](https://pubmed.ncbi.nlm.nih.gov/5538935/)
- L. Oksanen, T. Oksanen, The logic and realism of the hypothesis of exploitation ecosystems. *Am. Nat.* **155**, 703–723 (2000). doi: [10.1086/303354](https://doi.org/10.1086/303354); pmid: [10805639](https://pubmed.ncbi.nlm.nih.gov/10805639/)
- K. S. McCann, *Food Webs (MPB-50)* (Princeton Univ. Press, Princeton, NJ, 2011).
- R. Arditi, L. Ginzburg, *How Species Interact: Altering the Standard View on Trophic Ecology* (Oxford Univ. Press, Oxford, 2012).
- A. R. E. Sinclair, S. Mduma, J. S. Brashares, Patterns of predation in a diverse predator-prey system. *Nature* **425**, 288–290 (2003). doi: [10.1038/nature01934](https://doi.org/10.1038/nature01934); pmid: [13679915](https://pubmed.ncbi.nlm.nih.gov/13679915/)
- N. Owen-Smith, M. G. L. Mills, Predator-prey size relationships in an African large-mammal food web. *J. Anim. Ecol.* **77**, 173–183 (2008). doi: [10.1111/j.1365-2656.2007.01314.x](https://doi.org/10.1111/j.1365-2656.2007.01314.x); pmid: [18177336](https://pubmed.ncbi.nlm.nih.gov/18177336/)
- H. Cyr, M. L. Pace, Allometric theory: Extrapolations from individuals to communities. *Ecology* **74**, 1234–1245 (1993). doi: [10.2307/1940493](https://doi.org/10.2307/1940493)
- C. Carbone, J. L. Gittleman, A common rule for the scaling of carnivore density. *Science* **295**, 2273–2276 (2002). doi: [10.1126/science.1067994](https://doi.org/10.1126/science.1067994); pmid: [11910114](https://pubmed.ncbi.nlm.nih.gov/11910114/)
- A. J. Lotka, *Elements of Physical Biology* (Dover, New York, 1924).
- V. Volterra, Fluctuations in the abundance of a species considered mathematically. *Nature* **118**, 558–560 (1926). doi: [10.1038/118558a0](https://doi.org/10.1038/118558a0)
- J. P. DeLong, D. A. Vasseur, A dynamic explanation of size-density scaling in carnivores. *Ecology* **93**, 470–476 (2012). doi: [10.1890/11-1138.1](https://doi.org/10.1890/11-1138.1); pmid: [22624202](https://pubmed.ncbi.nlm.nih.gov/22624202/)
- S. Pawar, A. I. Dell, V. M. Savage, Dimensionality of consumer search space drives trophic interaction strengths. *Nature* **486**, 485–489 (2012). pmid: [22722834](https://pubmed.ncbi.nlm.nih.gov/22722834/)
- C. Melis *et al.*, Predation has a greater impact in less productive environments: Variation in roe deer, *Capreolus capreolus*, population density across Europe. *Glob. Ecol. Biogeogr.* **18**, 724–734 (2009). doi: [10.1111/j.1466-8238.2009.00480.x](https://doi.org/10.1111/j.1466-8238.2009.00480.x)
- G. Wang *et al.*, Density dependence in northern ungulates: Interactions with predation and resources. *Popul. Ecol.* **51**, 123–132 (2009). doi: [10.1007/s10144-008-0095-3](https://doi.org/10.1007/s10144-008-0095-3)
- A. Treves, A. J. Plumptre, L. T. B. Hunter, J. Ziwa, Identifying a potential lion *Panthera leo* stronghold in Queen Elizabeth National Park, Uganda, and Parc National des Virunga, Democratic Republic of Congo. *Oryx* **43**, 60–66 (2009). doi: [10.1017/S003060530700124X](https://doi.org/10.1017/S003060530700124X)
- C. Carbone, N. Pettorelli, P. A. Stephens, The bigger they come, the harder they fall: Body size and prey abundance influence predator-prey ratios. *Biol. Lett.* **7**, 312–315 (2011). doi: [10.1098/rsbl.2010.0996](https://doi.org/10.1098/rsbl.2010.0996); pmid: [21106569](https://pubmed.ncbi.nlm.nih.gov/21106569/)
- B. Jedrzejewska, W. Jedrzejewski, *Predation in Vertebrate Communities: The Białowieża Primeval Forest as a Case Study* (Springer, Berlin, 1998), vol. 135.
- E. Jeppesen, J. Pedersen, M. Sondergaard, T. Lauridsen, F. Landkildehus, Trophic structure, species richness and biodiversity in Danish lakes: Changes along a phosphorus gradient. *Freshw. Biol.* **45**, 201–218 (2000). doi: [10.1046/j.1365-2427.2000.00675.x](https://doi.org/10.1046/j.1365-2427.2000.00675.x)
- Q. Dortch, T. T. Packard, Differences in biomass structure between oligotrophic and eutrophic marine ecosystems. *Deep-Sea Res. A. Oceanogr. Res. Pap.* **36**, 223–240 (1989). doi: [10.1016/0198-0149\(89\)90135-0](https://doi.org/10.1016/0198-0149(89)90135-0)
- P. Legendre, L. F. Legendre, *Numerical Ecology* (Elsevier, Amsterdam, 2012), vol. 24.
- K. J. Niklas, B. J. Enquist, Biomass allocation and growth data of seeded plants data set, Oak Ridge National Laboratory Distributed Active Archive Center, Oak Ridge, TN (2004), [www.daac.ornl.gov](http://www.daac.ornl.gov).
- K. Banse, S. Mosher, Adult body mass and annual production/biomass relationships of field populations. *Ecol. Monogr.* **50**, 355–379 (1980). doi: [10.2307/2937256](https://doi.org/10.2307/2937256)
- R. H. Peters, *The Ecological Implications of Body Size* (Cambridge Studies in Ecology, Cambridge Univ. Press, Cambridge, ed. 1, 1983).
- F. Fenchel, Intrinsic rate of natural increase: The relationship with body size. *Oecologia* **14**, 317–326 (1974). doi: [10.1007/BF00384576](https://doi.org/10.1007/BF00384576)
- T. J. Case, On the evolution and adaptive significance of postnatal growth rates in the terrestrial vertebrates. *Q. Rev. Biol.* **53**, 243–282 (1978). doi: [10.1086/410622](https://doi.org/10.1086/410622); pmid: [362471](https://pubmed.ncbi.nlm.nih.gov/362471/)

71. S. K. M. Ernest *et al.*, Thermodynamic and metabolic effects on the scaling of production and population energy use. *Ecol. Lett.* **6**, 990–995 (2003). doi: [10.1046/j.1461-0248.2003.00526.x](https://doi.org/10.1046/j.1461-0248.2003.00526.x)
72. J. M. Grady, B. J. Enquist, E. Dettweiler-Robinson, N. A. Wright, F. A. Smith, Evidence for mesothermy in dinosaurs. *Science* **344**, 1268–1272 (2014). pmid: [24926017](https://doi.org/10.1126/science.1249261)
73. L. von Bertalanffy, Quantitative laws in metabolism and growth. *Q. Rev. Biol.* **32**, 217–231 (1957). doi: [10.1086/401873](https://doi.org/10.1086/401873); pmid: [13485376](https://doi.org/10.1086/3508076)
74. G. B. West, J. H. Brown, B. J. Enquist, A general model for ontogenetic growth. *Nature* **413**, 628–631 (2001). doi: [10.1038/3508076](https://doi.org/10.1038/3508076); pmid: [1675785](https://doi.org/10.1038/1675785)
75. A. M. Makarieva, V. G. Gorshkov, B.-L. Li, Ontogenetic growth: Models and theory. *Ecol. Model.* **176**, 15–26 (2004). doi: [10.1016/j.ecolmodel.2003.09.037](https://doi.org/10.1016/j.ecolmodel.2003.09.037)
76. C. Hou *et al.*, Energy uptake and allocation during ontogeny. *Science* **322**, 736–739 (2008). doi: [10.1126/science.1162302](https://doi.org/10.1126/science.1162302); pmid: [18974352](https://doi.org/10.1126/science.1162302)
77. J. P. DeLong, J. G. Okie, M. E. Moses, R. M. Sibly, J. H. Brown, Shifts in metabolic scaling, production, and efficiency across major evolutionary transitions of life. *Proc. Natl. Acad. Sci. U.S.A.* **107**, 12941–12945 (2010). doi: [10.1073/pnas.1007783107](https://doi.org/10.1073/pnas.1007783107); pmid: [20616006](https://doi.org/10.1073/pnas.1007783107)
78. R. M. Sibly, D. Barker, M. C. Denham, J. Hone, M. Pagel, On the regulation of populations of mammals, birds, fish, and insects. *Science* **309**, 607–610 (2005). doi: [10.1126/science.1110760](https://doi.org/10.1126/science.1110760); pmid: [16040705](https://doi.org/10.1126/science.1110760)
79. B. W. Brook, C. J. Bradshaw, Strength of evidence for density dependence in abundance time series of 1198 species. *Ecology* **87**, 1445–1451 (2006). doi: [10.1890/0012-9658\(2006\)87\[1445:SOEFDD\]2.0.CO;2](https://doi.org/10.1890/0012-9658(2006)87[1445:SOEFDD]2.0.CO;2); pmid: [16869419](https://doi.org/10.1890/0012-9658(2006)87[1445:SOEFDD]2.0.CO;2)
80. N. B. Goodwin, A. Grant, A. L. Perry, N. K. Dulvy, J. D. Reynolds, Life history correlates of density-dependent recruitment in marine fishes. *Can. J. Fish. Aquat. Sci.* **63**, 494–509 (2006). doi: [10.1139/f05-234](https://doi.org/10.1139/f05-234)
81. J. P. DeLong, T. C. Hanley, D. A. Vasseur, Competition and the density dependence of metabolic rates. *J. Anim. Ecol.* **83**, 51–58 (2014). doi: [10.1111/1365-2656.12065](https://doi.org/10.1111/1365-2656.12065); pmid: [23565624](https://doi.org/10.1111/1365-2656.12065)
82. R. A. Duursma *et al.*, Self-shading affects allometric scaling in trees. *Funct. Ecol.* **24**, 723–730 (2010). doi: [10.1111/j.1365-2435.2010.01690.x](https://doi.org/10.1111/j.1365-2435.2010.01690.x)
83. G. B. West, B. J. Enquist, J. H. Brown, A general quantitative theory of forest structure and dynamics. *Proc. Natl. Acad. Sci. U.S.A.* **106**, 7040–7045 (2009). doi: [10.1073/pnas.0812294106](https://doi.org/10.1073/pnas.0812294106); pmid: [19363160](https://doi.org/10.1073/pnas.0812294106)
84. N. G. Hairston Jr., N. G. Hairston Sr., Cause-effect relationships in energy flow, trophic structure, and interspecific interactions. *Am. Nat.* **142**, 379–411 (1993). doi: [10.1086/285546](https://doi.org/10.1086/285546)
85. A. J. Kerckhoff, B. J. Enquist, Ecosystem allometry: The scaling of nutrient stocks and primary productivity across plant communities. *Ecol. Lett.* **9**, 419–427 (2006). doi: [10.1111/j.1461-0248.2006.00888.x](https://doi.org/10.1111/j.1461-0248.2006.00888.x); pmid: [16623727](https://doi.org/10.1111/j.1461-0248.2006.00888.x)
86. S. Watson, E. McCauley, Contrasting patterns of net-and nanoplankton production and biomass among lakes. *Can. J. Fish. Aquat. Sci.* **45**, 915–920 (1988). doi: [10.1139/f88-112](https://doi.org/10.1139/f88-112)
87. C. Packer *et al.*, Ecological change, group territoriality, and population dynamics in Serengeti lions. *Science* **307**, 390–393 (2005). doi: [10.1126/science.1105122](https://doi.org/10.1126/science.1105122); pmid: [15662005](https://doi.org/10.1126/science.1105122)
88. J. M. Fryxell, A. Mosser, A. R. E. Sinclair, C. Packer, Group formation stabilizes predator-prey dynamics. *Nature* **449**, 1041–1043 (2007). doi: [10.1038/nature06177](https://doi.org/10.1038/nature06177); pmid: [17960242](https://doi.org/10.1038/nature06177)
89. W. E. Ricker, Linear regressions in fishery research. *J. Fish. Board Can.* **30**, 409–434 (1973). doi: [10.1139/f73-072](https://doi.org/10.1139/f73-072)
90. B. H. McArdle, The structural relationship: Regression in biology. *Can. J. Zool.* **66**, 2329–2339 (1988). doi: [10.1139/z88-348](https://doi.org/10.1139/z88-348)
91. R. R. Sokal, F. J. Rohlf, *Biometry* (Freeman, New York, ed. 3, 1995).
92. P. Jolicoeur, Bivariate allometry: Interval estimation of the slopes of the ordinary and standardized normal major axes and structural relationship. *J. Theor. Biol.* **144**, 275–285 (1990). doi: [10.1016/S0022-5193\(05\)80326-1](https://doi.org/10.1016/S0022-5193(05)80326-1)
93. D. I. Warton, I. J. Wright, D. S. Falster, M. Westoby, Bivariate line-fitting methods for allometry. *Biol. Rev. Camb. Philos. Soc.* **81**, 259–291 (2006). doi: [10.1017/S1464793106007007](https://doi.org/10.1017/S1464793106007007); pmid: [16573844](https://doi.org/10.1017/S1464793106007007)
94. R. J. Smith, Use and misuse of the reduced major axis for line-fitting. *Am. J. Phys. Anthropol.* **140**, 476–486 (2009). doi: [10.1002/ajpa.21090](https://doi.org/10.1002/ajpa.21090); pmid: [19425097](https://doi.org/10.1002/ajpa.21090)
95. E. P. White, X. Xiao, N. Isaac, R. M. Sibly, "Methodological tools," in *Metabolic Ecology: A Scaling Approach*. (2012), pp. 7–20.
96. C. R. White, Allometric estimation of metabolic rates in animals. *Comp. Biochem. Physiol. A Mol. Integr. Physiol.* **158**, 346–357 (2011). doi: [10.1016/j.cbpa.2010.10.004](https://doi.org/10.1016/j.cbpa.2010.10.004); pmid: [20937406](https://doi.org/10.1016/j.cbpa.2010.10.004)
97. K. Nowell, P. Jackson, *Wild Cats: Status Survey and Conservation Action Plan* (IUCN/SSC Cat Specialist Group, Gland, Switzerland, 1996).
98. P. M. Gros, M. J. Kelly, T. M. Caro, Estimating carnivore densities for conservation purposes: Indirect methods compared to baseline demographic data. *Oikos* **77**, 197 (1996). doi: [10.2307/3546058](https://doi.org/10.2307/3546058)
99. J. Kalfi, *Limnology: Inland Water Ecosystems* (Prentice Hall, Upper Saddle River, NJ, 2002), vol. 592.
100. E. McCauley, in *A Manual on Methods for the Assessment of Secondary Productivity in Fresh Waters* (Blackwell Scientific, Oxford, 1984), pp. 228–265.
101. G. Harris, *Phytoplankton Ecology-Structure, Function and Fluctuation* (Chapman and Hall, New York, 1986).
102. N. Billington, A comparison of three methods of measuring phytoplankton biomass on a daily and seasonal basis. *Hydrobiologia* **226**, 1–15 (1991). doi: [10.1007/BF00007775](https://doi.org/10.1007/BF00007775)
103. J. S. Singh, W. K. Lauenroth, R. K. Steinhorst, Review and assessment of various techniques for estimating net aerial primary production in grasslands from harvest data. *Bot. Rev.* **41**, 181–232 (1975). doi: [10.1007/BF02860829](https://doi.org/10.1007/BF02860829)
104. D. A. Clark *et al.*, Measuring net primary production in forests: Concepts and field methods. *Ecol. Appl.* **11**, 356–370 (2001). doi: [10.1890/1051-0761\(2001\)011\[0356:MNPPIF\]2.0.CO;2](https://doi.org/10.1890/1051-0761(2001)011[0356:MNPPIF]2.0.CO;2)
105. S. P. Long, P. R. Hutchin, Primary production in grasslands and coniferous forests with climate change: An overview. *Ecol. Appl.* **1**, 139–156 (1991). doi: [10.2307/1941807](https://doi.org/10.2307/1941807)
106. C. Plante, J. A. Downing, Empirical evidence for differences among methods for calculating secondary production. *J. N. Am. Benthol. Soc.* **9**, 9–16 (1990). doi: [10.2307/1467929](https://doi.org/10.2307/1467929)
107. E. P. White, B. J. Enquist, J. L. Green, On estimating the exponent of power-law frequency distributions. *Ecology* **89**, 905–912 (2008). doi: [10.1890/07-1288.1](https://doi.org/10.1890/07-1288.1); pmid: [18481513](https://doi.org/10.1890/07-1288.1)
108. A. Claustre, C. R. Shalizi, M. E. Newman, Power-law distributions in empirical data. *SIAM Rev.* **51**, 661–703 (2009). doi: [10.1137/070710111](https://doi.org/10.1137/070710111)
109. S. Nee, N. Colegrave, S. A. West, A. Grafen, The illusion of invariant quantities in life histories. *Science* **309**, 1236–1239 (2005). doi: [10.1126/science.1114488](https://doi.org/10.1126/science.1114488); pmid: [16109879](https://doi.org/10.1126/science.1114488)
110. M. J. Coe, D. H. Cumming, J. Phillipson, Biomass and production of large African herbivores in relation to rainfall and primary production. *Oecologia* **22**, 341–354 (1976). doi: [10.1007/BF00345312](https://doi.org/10.1007/BF00345312)
111. H. Fritz, P. Duncan, On the carrying capacity for large ungulates of African savanna ecosystems. *Proc. R. Soc. London Ser. B* **256**, 77–82 (1994). doi: [10.1098/rspb.1994.0052](https://doi.org/10.1098/rspb.1994.0052); pmid: [8008761](https://doi.org/10.1098/rspb.1994.0052)
112. MAPA Project, MAPA Project, (2011), [www.mapaproject.org/](http://www.mapaproject.org/)
113. ALERT, African Lion and Environmental Research Trust (2011), [www.lionalert.org/](http://www.lionalert.org/)
114. J. Damuth, Interspecific allometry of population density in mammals and other animals: The independence of body mass and population energy-use. *Biol. J. Linn. Soc. Lond.* **31**, 193–246 (1987). doi: [10.1111/j.1095-8312.1987.tb01990.x](https://doi.org/10.1111/j.1095-8312.1987.tb01990.x)
115. R. East, IUCN/SSC Antelope Specialist Group, *African Antelope Database 1998* (IUCN, Gland, Switzerland, and Cambridge, UK, 1999).
116. R. J. Power, R. X. Shem Compion, Lion predation on elephants in the Savuti, Chobe National Park, Botswana. *Afr. Zool.* **44**, 36–44 (2009). doi: [10.3377/004.044.0104](https://doi.org/10.3377/004.044.0104)
117. J. M. Fryxell, J. Grever, A. R. E. Sinclair, Why are migratory ungulates so abundant? *Am. Nat.* **131**, 781–798 (1988). doi: [10.1086/284822](https://doi.org/10.1086/284822)
118. C. Kiffner, B. Meyer, M. Muhlenberg, M. Waltert, Plenty of prey, few predators: What limits lions *Panthera Leo* in Katavi National Park, Western Tanzania? *Oryx* **43**, 52–59 (2009). doi: [10.1017/S0030605309002335](https://doi.org/10.1017/S0030605309002335)
119. V. J. Wilson, *Mammals of the Wankie National Park, Rhodesia* (Trustees of the National Museums and Monuments of Rhodesia, Salisbury, Rhodesia, 1975).
120. L. D. Harris, "An ecological description of a semi-arid East African ecosystem," *Range Science Department Science Series* (11, Colorado State University, Fort Collins, CO, 1972).
121. H. F. Lamprey, The Tarangire game reserve. *Tanganyika Not. Record.* **60**, 10–22 (1963).
122. M. G. L. Mills, *Kalahari Hyenas: Comparative Behavioral Ecology of Two Species* (Blackburn, Caldwell, NJ, 1990).
123. D. I. Warton, R. A. Duursma, D. S. Falster, S. Taskinen, smatr 3—an R package for estimation and inference about allometric lines. *Methods Ecol. Evol.* **3**, 257–259 (2012). doi: [10.1111/j.2041-210X.2011.00153.x](https://doi.org/10.1111/j.2041-210X.2011.00153.x)
124. T. X. Luo, thesis, Chinese Academy of Sciences, Beijing, China (1996).
125. J. Ni, X.-S. Zhang, J. M. Scurlock, Synthesis and analysis of biomass and net primary productivity in Chinese forests. *Ann. For. Sci.* **58**, 351–384 (2001). doi: [10.1051/forest:2001131](https://doi.org/10.1051/forest:2001131)
126. A. M. Makarieva *et al.*, Mean mass-specific metabolic rates are strikingly similar across life's major domains: Evidence for life's metabolic optimum. *Proc. Natl. Acad. Sci. U.S.A.* **105**, 16994–16999 (2008). doi: [10.1073/pnas.0802148105](https://doi.org/10.1073/pnas.0802148105); pmid: [18952839](https://doi.org/10.1073/pnas.0802148105)
127. V. M. Savage, J. F. Gillooly, J. H. Brown, G. B. West, E. L. Charnov, Effects of body size and temperature on population growth. *Am. Nat.* **163**, 429–441 (2004). doi: [10.1086/381872](https://doi.org/10.1086/381872); pmid: [15026978](https://doi.org/10.1086/381872)
128. R. P. Duncan, D. M. Forsyth, J. H. Hone, Testing the metabolic theory of ecology: Allometric scaling exponents in mammals. *Ecology* **88**, 324–333 (2007). doi: [10.1890/0012-9658\(2007\)88\[324TTMTOE\]2.0.CO;2](https://doi.org/10.1890/0012-9658(2007)88[324TTMTOE]2.0.CO;2); pmid: [17479751](https://doi.org/10.1890/0012-9658(2007)88[324TTMTOE]2.0.CO;2)
129. W. F. Fagan, H. J. Lynch, B. R. Noon, Pitfalls and challenges of estimating population growth rate from empirical data: Consequences for allometric scaling relations. *Oikos* **119**, 455–464 (2010). doi: [10.1111/j.1600-0706.2009.18002.x](https://doi.org/10.1111/j.1600-0706.2009.18002.x)
130. H. M. Pereira, G. C. Daily, Modeling biodiversity dynamics in countryside landscapes. *Ecology* **87**, 1877–1885 (2006). doi: [10.1890/0012-9658\(2006\)87\[1877:MBDICL\]2.0.CO;2](https://doi.org/10.1890/0012-9658(2006)87[1877:MBDICL]2.0.CO;2); pmid: [16937624](https://doi.org/10.1890/0012-9658(2006)87[1877:MBDICL]2.0.CO;2)

**ACKNOWLEDGMENTS**

We thank N. Owen-Smith, L. Glass, J. H. Brown, V. M. Savage, J. P. Lessard, J. P. DeLong, J. M. Grady, and three anonymous reviewers for helpful comments on earlier drafts; X. Irigoien, S. K. M. Ernest, and H. Cyr for providing data; S. N. Driscoll for mapping assistance; and C. Miki for database assistance. I.A.H. was supported by a Natural Sciences and Engineering Research Council of Canada CGS-D fellowship. M.L. was supported by the TULIP Laboratory of Excellence (ANR-10-LABX-41). Research at Perimeter Institute was supported by the Government of Canada through Industry Canada and by the Province of Ontario through the Ministry of Research and Innovation. Data are available in the supplementary materials at Science Online.

**SUPPLEMENTARY MATERIALS**

[www.sciencemag.org/content/349/6252/aac6284/suppl/DC1](http://www.sciencemag.org/content/349/6252/aac6284/suppl/DC1)  
Supplementary Text  
Tables S1 to S5  
Appendices S1 and S2  
References (131–144)  
Database S1  
21 May 2015; accepted 3 August 2015  
10.1126/science.aac6284